JOURNAL OF CATALYSIS 116, 195–221 (1989)

Higher Alcohol and Oxygenate Synthesis over Cesium-Doped Cu/ZnO Catalysts

JOHN G. NUNAN,[1] CHARLES E. BOGDAN,[2] KAMIL KLIER, KEVIN J. SMITH,[3] CHYI-WOEI YOUNG,[4] AND RICHARD G. HERMAN

Zettlemoyer Center for Surface Studies and Department of Chemistry, Lehigh University, Bethlehem, Pennsylvania 18015

Received June 22, 1988

The synthesis of higher (C_2^+) alcohols and esters has been studied over cesium-doped Cu/ZnO catalysts. Under higher alcohol synthesis conditions, e.g., 583 K, 7.6 MPa, and gas hourly space velocity = 3260 liters (STP)/kg cat/hr with a $H_2/CO = 0.45$ synthesis gas, the presence of cesium promoted the formation of higher oxygenates, especially 2-methyl-1-propanol. The yields of products passed through distinct maxima at cesium nominal concentrations of 0.3–0.5%. These nominal concentrations generated optimum surface cesium concentrations of 15–25%. Under the reaction conditions employed, the principal role of cesium was to increase the ethanol synthesis rate and to provide an even greater enhancement in the rate of ethanol conversion to 1-propanol and subsequently to higher alcohols. To obtain insight into the mechanism of the carbon chain growth, e.g., $C_1 \rightarrow C_2$, $C_2 \rightarrow C_3$, and linear versus branched carbon chain growth, a ^{13}C-NMR study of the C_2–C_4 products formed over Cu/ZnO and 0.4 mol% Cs/Cu/ZnO catalysts was performed. Separate injections into the CO/H_2 synthesis gas of methanol and ethanol with natural-abundance ^{13}C and enriched by ^{13}C in specific positions showed that (i) lower alcohols were incorporated into the synthesis to form higher alcohols; (ii) carbon chain growth occurred in a stepwise manner dominated by the addition of oxygenated C_1 intermediates at the β carbons of the oxygenated C_n ($n \geq 2$) intermediates but also proceeding via linear addition $C_n + C_1$ ($n \geq 1$); and (iii) the presence of cesium had a dramatic effect on the reaction mechanism and promoted greatly the synthesis rates. The mechanistic effects of the alkali dopant were most pronounced in the $C_2 \rightarrow C_3$ step. Over the Cu/ZnO catalyst, injection of ethanol produced 1-propanol via linear chain growth, i.e., $CH_3{}^{13}CH_2OH + CO/H_2 \rightarrow CH_3{}^{13}CH_2CH_2OH$. The presence of Cs effected a mechanistic switch and promoted *β-carbon addition*, $CH_3{}^{13}CH_2OH + CO/H_2 \rightarrow {}^{13}CH_3CH_2CH_2OH$. The position of the ^{13}C label in the CH_3 group of propanol provides evidence for retention of oxygen associated with the C_1 intermediate, formed from CO/H_2, and loss of oxygen associated with the $^{13}CH_2OH$ group of ethanol. Mechanistically, such a retention is favored by a β-ketoalkoxide intermediate that is bonded to the cesium centers via its anionic oxygen. This unique mechanism is termed herein as *aldol coupling with oxygen retention reversal* and is specific to the presence of the cesium salt dopant. Higher alcohol synthetic steps $C_2 + C_2$ and $C_n + C_m$ ($n \geq 3$, $m = 1, 2, 3$) were also analyzed. Both oxygen retention reversal and normal oxygen retention were observed in coupling reactions leading to the higher-molecular-weight products ($m + n > 3$), and this observation is attributed to steric effects favoring the *cis* conformation of the β-alkoxide followed by rejection of either of its two oxygens. © 1989 Academic Press, Inc.

INTRODUCTION

In previous papers (*1–3*), the present authors reported the promotion of methanol and $C_1 \rightarrow C_2$ oxygenate synthesis over a range of cesium-doped and undoped Cu/ZnO catalysts. In that study, typical methanol synthesis conditions were employed [e.g., $H_2/CO = 2.33$, gas hourly space ve-

[1] Present address: Allied Signal, P.O. Box 5016, Des Plaines, IL 60017.

[2] Present address: J. T. Baker, Inc., 222 Red School Lane, Phillipsburg, NJ 08865.

[3] Present address: Department of Chemical Engineering and Applied Chemistry, University of Toronto, Toronto M5S 1A4, Canada.

[4] Present address: New Materials R&D Department T6, China Steel Corp., P.O. Box 47-29, Kaohsiung 81233, Republic of China.

0021-9517/89 $3.00
Copyright © 1989 by Academic Press, Inc.
All rights of reproduction in any form reserved.

locity = 6120 liters (STP)/kg cat/hr, 7.6 MPa, 523 K], and five points were demonstrated:

1. Surface doping of the Cu/ZnO catalysts by cesium compounds promoted the synthesis of methanol, methyl formate, and ethanol. The yields of methanol and methyl formate passed through distinct maxima at cesium loadings of 0.8 and 1.2 mol%, respectively, while the rate of ethanol formation increased up to a concentration of 1.5 mol% cesium, after which it remained nearly constant (*1, 2*).

2. The rate of methanol synthesis was enhanced under the above conditions by a factor of up to 2.2 by doping the surface of the catalyst with cesium while maintaining the methanol selectivity at greater than 98.9 mol% of the total oxygenate product (*1*).

3. The water gas shift reaction was also promoted by the factor up to 2.2 by cesium doping (*3*).

4. Methyl formate was shown to be formed by direct carbonylation of methanol with CO, and this reaction was at equilibrium under higher alcohol synthesis conditions, i.e., with CO-rich synthesis gas mixtures such as $H_2/CO = 0.45$, at temperatures greater than 523 K, and with GHSV = 3260 liters (STP)/kg cat/hr (*2*); and

5. The direct carbon source for ethanol and 1-propanol synthesis was found to be methanol (*2*).

In regard to the last point, it was determined that reaction mechanisms for chain growth involving direct CO insertion into adsorbed surface species were not important over the Cu/ZnO catalysts doped with alkali or undoped. Such insertion mechanisms have been proposed earlier and these include CO insertion into the C–O bond of C_nOH to give C_nCOOH, followed by hydrogenation to give $C_{n+1}OH$ (*4*); CO insertion into a metal alkoxide followed by rearrangement to give metal carboxylate, which is subsequently hydrogenated to the corresponding alcohol (*5, 6*); CO insertion into the M–C bond of a surface-bound aldehyde followed by rearrangement and hydrogenation to the alcohol (*7*); and CO insertion into the M–C bond of surface CH_x fragments (*8, 9*), as originally proposed for homogeneous CO organometallic catalysis (*10*). Other proposals included the suggestion that higher alcohols are formed via condensation of lower alcohols (*11, 12*). Related to this condensation mechanism is the aldol condensation mechanism proposed by Morgan *et al.* (*13*) and Fox *et al.* (*14*), whereby the dehydrogenated form of the alcohol, i.e., aldehyde for a primary alcohol or ketone for secondary alcohol, is the reactant in the condensation reaction. If the alcohol and aldehyde are in equilibrium, either reactant can be considered to be the direct carbon source for higher alcohol synthesis. The details of the aldol condensation-based mechanisms are discussed herein after the patterns of isotope label flows in the higher alcohol synthesis have been presented.

In addition to methanol and higher primary alcohols, the products obtained over the Cu/ZnO-based catalysts include aldehydes, ketones, esters, and secondary alcohols. Since both ZnO and copper are well-known hydrogenation–dehydrogenation catalysts (*15–20*), the alcohols and the corresponding dehydrogenated aldehyde or ketone products are expected to coexist, especially in hydrogen-poor mixtures. Esters are also observed, among which methyl esters are dominant products (*6, 21*). Several mechanisms leading to the formation of esters are possible, and these include (a) a Cannizzaro-type condensation of two aldehydes, as proposed by Frolich and Cryder (*11*), and (b) coupling between a surface alkoxide and an aldehyde with resultant hydride elimination, as proposed by Vedage *et al.* (6) and Elliott and Pennella (*21*).

The types of catalysts studied here are derived from Cu/ZnO methanol synthesis catalysts that have been modified by the addition of compounds of heavy alkali metal ions and by employing the reaction conditions under which higher alcohol synthesis

is favored. The introduction of alkali metal ions such as cesium was prompted by the desire to increase the basicity of the catalyst surface so that aldol condensation reactions became favored. Vedage *et al.* (*6*) demonstrated that the rates and selectivities for higher alcohols increased in ion-specific fashion with the increase of size of the alkali ion such that the effects of Cs promotion were approximately twofold the promotion effects of K. The catalysts studied in the current investigation consisted of Cu/ZnO and Cs-promoted Cu/ZnO catalysts. These catalysts are similar in type [as defined by Natta *et al.* (*5*) in terms of being *neither* simply modified Fischer–Tropsch catalysts nor isosynthesis catalysts] to the K/Mn/Zn/Cr catalysts studied by Frolich and Cryder (*11*) and the alkali/MnO/Cr_2O_3 catalyst utilized by Morgan *et al.* (*13*). However, the current Cu/ZnO-based catalysts have been modified and optimized via preparation techniques and precursors formed so that their activities under mild conditions far exceed those reported for the Mn-containing catalysts (*11, 13*).

The purpose of the present investigation was to study the effects of cesium doping on the synthesis rates, mechanism, and ensuing selectivities to oxygenates produced under high alcohol synthesis reaction conditions. Special attention was directed toward the specific effect of cesium on the chain growth processes that led to linear C_3–C_6 and branched C_4–C_6 primary alcohols. An important tool employed in the present investigation was the use of ^{13}C-NMR spectroscopy to follow the incorporation of lower alcohols into higher-molecular-weight products.

EXPERIMENTAL

Catalyst preparation. Preparation of the binary Cu/ZnO catalysts involved the initial precipitation of the hydroxycarbonate precursor aurichalcite $[Cu_{1.5}Zn_{3.5}(OH)_6(CO_3)_2]$ by a previously described procedure (*22, 23*), followed by stepwise calcination to 623 K to give the corresponding mixture of oxides, CuO/ZnO = 30/70. Cesium doping with the formate salt CsOOCH was effected by adding 2.5 g of the calcined pelletized sieved 0.85- to 2.0-mm catalyst particles to 25 ml of N_2-purged aqueous CsOOCH solution at 323 K. The solution was then evaporated to dryness under flowing N_2, and the resulting cesium-doped CuO/ZnO catalyst precursor was charged into the reactor for the determination of activity. Most catalytic testing was carried out with 0.3–0.5 mol% CsOOCH/Cu/ZnO catalysts. Quantitative X-ray photoelectron spectroscopic (XPS) analysis showed that the cesium salt was dispersed in a submonolayer corresponding to cesium surface concentrations of 15–25% on these catalysts (*6*). Before pressurizing the reactor, the catalyst was reduced with a 2 mol% H_2 in N_2 mixture at 523 K. Reduction was followed by monitoring water content in the exit gas using gas chromatographic analysis and was terminated when a sudden drop in the production of water was observed.

Determination of catalyst activity and selectivity in alcohol synthesis. Catalytic testing with a $H_2/CO = 0.45$ synthesis gas was carried out in fixed-bed continuous-flow 316 stainless-steel reactors operating at a total pressure of 7.6 MPa. A schematic of one of the two testing systems utilized is shown in Fig. 1. Reactor construction and mode of operation have been described in detail previously (*22, 24*). Portions of 2.45 g of the catalyst were used. The catalyst was diluted with three times its volume of 3-mm Pyrex beads and formed into a bed in the central portion of the reactor. The reactor was operated 24 hr/day in an automated fashion and the long-term performance of each catalyst was determined in reaction runs of up to 1000 hr. Results of the long-term activity tests will be reported elsewhere. The initial activities reported here are representative of the long-term performance of the optimized catalysts.

The exit product mixture from the reactor was sampled every 20–60 min using an in-line automated heated sampling valve

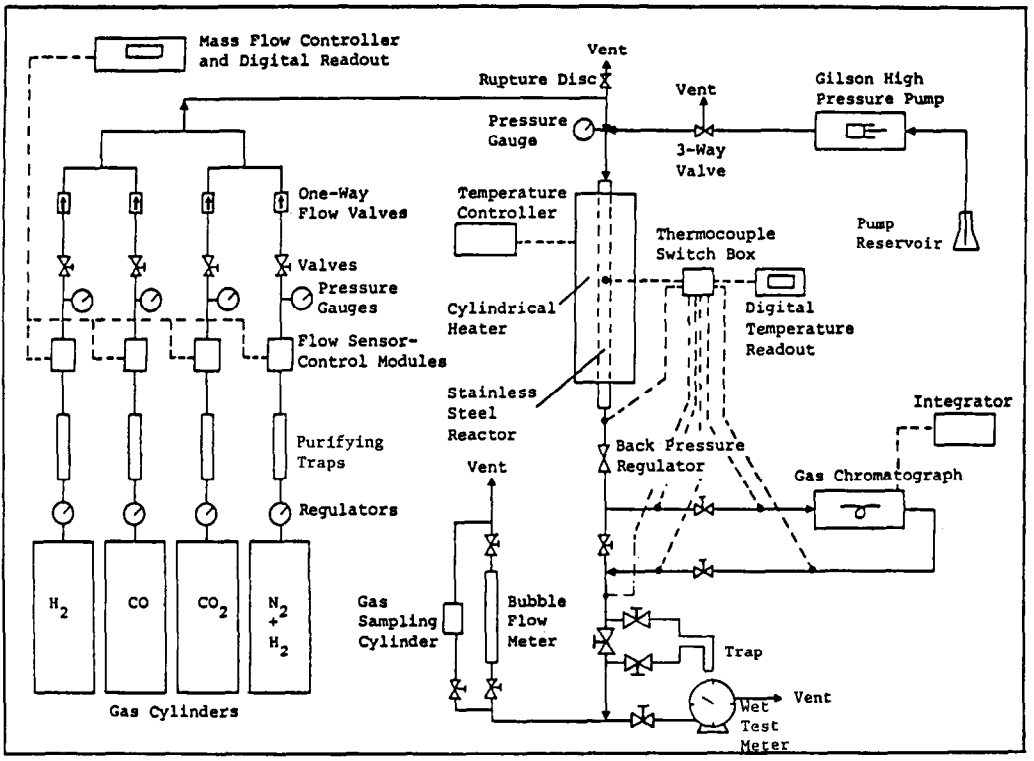

FIG. 1. Schematic of the reactor systems used to test the alcohol synthesis catalysts. Note the high-pressure injection pump at the top of the reactor that was used to introduce ^{13}C-labeled alcohols into the H_2/CO reactants passing over the catalyst.

and analyzed in a Hewlett–Packard 5730A gas chromatograph that was coupled with a Hewlett–Packard Model 3388A integrator/controller. Reaction products were separated on Porapak Q columns and were identified by comparison of their retention times with those of known standards and also from their mass spectroscopic (MS) fragmentation patterns, as determined by a Finnegan 4021 GC/MS/Nova system. Coupled with the above on-line GC analyses was a more extensive analysis of the higher-molecular-weight liquid product that was collected in liquid nitrogen-cooled traps. This analysis was carried out with a film type SPB-1 wide-bore Supelco 60-m × 0.75-mm i.d. capillary column (1.0-μm film thickness) inserted in a Hewlett–Packard Model 5890 gas chromatograph. Hydrogen was excluded from the compositional analyses, and reported thermal response factors (*25*) were utilized to correct for the different thermal conductivities of the reaction products.

Catalytic activities and selectivities were determined in the temperature range 513–583 K at 7.6 MPa with $H_2/CO = 0.45$ synthesis gas. The gas hourly space velocity (GHSV) employed was 3260 liters (STP)/kg cat/hr. All experimental data were obtained under steady-state conditions that were usually maintained for 1–24 hr before changing the reaction conditions to obtain another set of data.

Introduction of ^{13}C-labeled compounds and ^{13}C-NMR analyses of the product. The reaction mechanisms leading to higher oxygenate synthesis were probed by injecting ^{13}C-enriched methanol and ethanol into the CO/H_2 synthesis gas. The individual ^{13}C-

enriched alcohols were introduced into the synthesis gas at the inlet of the reactor using a high-pressure continuous-feed Model 302 Gilson pump at the rate of 10 μl/min over the 2.45 g of Cs/Cu/ZnO catalyst. The reactor operated under steady-state synthesis conditions. During the ^{13}C-enriched alcohol injection experiments, and also during reference experiments utilizing injection of equal amounts of nonenriched alcohols, reaction products were collected in liquid nitrogen traps placed downstream from the back-pressure regulator and transferred to NMR tubes that were subsequently sealed. ^{13}C-NMR spectra were obtained with a JEOL FX90Q Fourier Transform NMR spectrometer using broadband proton decoupling. Quantitative measurements were made by suppressing the nuclear Overhauser effect using a gated decoupling sequence and by utilizing a 45° pulse angle with sufficiently long delays (>10 sec). Quantitative analysis of the ^{13}C concentration on each individual carbon of the product mixture was performed by peak height analysis, assuming similar half-peak widths for all peaks. Overall error of the ^{13}C concentration was relative 10% for the main products and 30% for the minor products.

Catalyst characterization. The catalysts were removed from the reactor under nitrogen, and were routinely examined for surface area by gas adsorption (*26*) and for phase composition and crystallite size by X-ray powder diffraction under nitrogen in airtight cells (*27*). Surface areas were obtained by the BET method using argon (0.168 nm^2/Ar atom). For these determinations, samples were charged under N_2 into the Pyrex analysis bulbs, evacuated overnight, and subsequently heated under a dynamic vacuum of 10^{-5} Torr for 1 h at 383 K prior to argon adsorption measurements at 77 K.

RESULTS

Cs/Cu/ZnO catalysts. Preliminary experiments that explored the effect of reaction temperature on the overall activity, selectivity, and stability of this catalyst established that 583 K was the optimum operating temperature under the present set of reaction conditions. The effect of adding cesium to the binary Cu/ZnO catalyst on the yields and selectivities of the main products formed at this temperature from H_2/CO = 0.45 synthesis gas is shown in Table 1. It is evident that doping the catalyst with cesium had a profound effect on the activity and selectivity of the catalyst. Table 1 demonstrates that small amounts of cesium led to dramatic increases in the yields of 2-methyl-1-propanol, 1-propanol, 1-butanol, and 2-methyl-1-butanol. Further incremented additions of cesium caused the

TABLE 1

Product Yields over the Cu/ZnO = 30/70 Catalyst and the Cesium-Doped Cu/ZnO Catalysts Obtained with a H_2/CO = 0.45 Synthesis Gas at 583 K and 7.6 MPa with GHSV = 3260 Liters (STP)/kg cat/hr

Catalyst	Product yield (g/kg cat/hr)										
	CO_2	Water	Alkanes[a]	Methanol	Ethanol	1-Propanol	2-Methyl-1-propanol	1-Butanol	2-Methyl-1-butanol	Methyl acetate	Others[b]
Undoped Cu/ZnO	367	1.3	16.8	204	22.6	10.1	20.7	3.4	8.6	10.5	34.1
0.25 mol% Cs/Cu/ZnO	412	1.3	16.2	181	22.7	29.6	28.9	8.6	11.5	9.6	53.8
0.34 mol% Cs/Cu/ZnO	403	1.7	13.4	157	17.0	38.1	48.6	8.2	15.5	9.9	82.3
0.43 mol% Cs/Cu/ZnO	430	1.3	14.0	162	18.2	24.1	33.6	4.6	11.7	7.4	37.3
1.5 mol% Cs/Cu/ZnO	403	0.04	4.3	213	8.1	18.0	4.8	—	—	1.0	10.9

[a] Alkanes = methane, ethane, and propane.

[b] Others = methyl esters, aldehydes, ketones, C_4^+ linear primary and secondary alcohols, C_4^+ branched primary and secondary alcohols, and methyl formate.

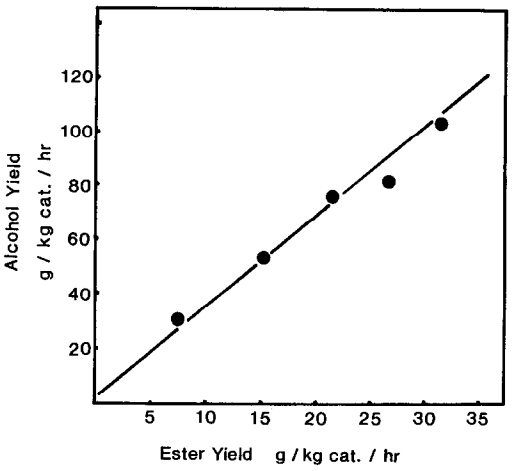

FIG. 2. Yields of ethanol + 1-propanol + 2-methyl-1-propanol vs the sum of the yields of the corresponding methyl esters (i.e., methyl acetate + methyl propanoate + methyl isobutanoate) produced over the undoped and cesium-doped Cu/ZnO= 30/70 mol% catalysts from H_2/CO = 0.45 synthesis gas at 583 K and 7.6 MPa with GHSV = 3260 liters (STP)/kg cat/hr. The individual points correspond, in ascending order, to 1.5, 0.0, 0.43, 0.25, and 0.34% Cs levels in the Cs/Cu/ZnO catalysts.

yields of these products to pass through distinct maxima between 0.30 and 0.40 mol% cesium in the catalyst. Higher levels of cesium concentrations caused a significant loss in catalytic activity.

The yield of methanol exhibited a behavior opposite to that of the higher alcohols. This arises because methanol was at or near equilibrium with the H_2 and CO reactants under the conditions employed, and its yield was at a minimum when the maximum amount of H_2 was consumed in higher oxygenate synthesis. In contrast to this, the yields of ethanol and methyl acetate were relatively unaffected by Cs concentrations up to 0.4 mol%, above which their yields decreased, as was observed with the higher alcohols. The compounds discussed above account for more than 80 wt% of the total higher oxygenate product. The balance of products consisted predominantly of the remaining methyl esters of carboxylic acids corresponding to the main higher alcohols, i.e., methylpropanoate, methylisobutanoate, and methylisopentanoate, and to a lesser extent the corresponding aldehydes. The effect of cesium doping on the selectivity to these esters and aldehydes was essentially the same as for the alcohols, and in fact the yields of esters closely followed those of the corresponding alcohols, as shown in Fig. 2.

The remaining side products included secondary alcohols and ketones, which also appeared in nearly constant ratios and were formed in amounts that were at maximum for 0.30–0.40% doping Cs levels. Other minor products are listed in Table 2 which contains and compares the product distributions obtained over the undoped Cu/ZnO catalyst and the 0.34 mol% Cs-doped Cu/ZnO catalyst. The effect of cesium doping on the hydrocarbon yield is also shown in Table 1. It is evident that doping the catalyst with cesium suppressed the yield of hydrocarbons, while the yield of CO_2 followed the same dependence on cesium doping levels as did the higher alcohols. Finally, the selectivity for higher oxygenate synthesis, relative to methanol, as a function of cesium concentration is shown in Table 3. It is observed that the higher oxygenate selectivity, defined in Table 3, increased from 35 wt% for the undoped catalyst to approximately 58 wt% for the optimally Cs-doped sample, i.e., 0.34 mol% Cs, by a factor of 1.66, as calculated from data in Table 1.

Incorporation of ^{13}C-enriched alcohols into the synthesis of higher alcohols. To gain insight into the carbon–carbon bond-forming steps that lead to higher alcohol synthesis, ^{13}C-enriched lower alcohols were injected into the CO/H_2 stream under steady-state conditions, and the collected product was analyzed by ^{13}C-NMR spectroscopy. In the first set of experiments, ethanol enriched in the C-1 position, i.e., $CH_3{}^{13}CH_2OH$, was used as the injected reactant alcohol. The ^{13}C-enriched ethanol was diluted with unlabeled ethanol to give an enrichment of the C-1 carbon of 20.2. The ^{13}C enrichment of each individual car-

TABLE 2

Comparison of the Product Compositions Obtained from $H_2/CO = 0.45$ Synthesis Gas at 583 K, 7.6 MPa, and GHSV = 3260 Liters (STP)/kg cat/hr over Binary Cu/ZnO and 0.34 mol% Cs/Cu/ZnO Catalysts

Product type	Product	Yield (g/kg cat/hr)	
		Undoped Cu/ZnO	0.34 mol% Cs/Cu/ZnO
Hydrocarbons, water, and CO_2	Methane	3.4	7.6
	Ethane	11.3	4.7
	Propane	2.1	1.1
	Water	1.3	1.7
	CO_2	367.	403.
Linear primary and secondary alcohols	Methanol	204.	157.
	Ethanol	22.6	17.0
	1-Propanol	10.1	38.1
	1-Butanol	3.4	8.2
	2-Butanol	0.7	1.8
	1-Pentanol	0.9	4.7
	3-Pentanol[a]	0.8	3.0
	1-Hexanol	2.0	5.5
Branched primary and secondary alcohols	2-Methyl-1-propanol	20.7	48.6
	2-Methyl-1-butanol	8.6	15.5
	3-Methyl-2-butanol	1.7	1.7
	2-Methyl-1-pentanol	5.1	12.4
	2-Methyl-3-pentanol	2.0	4.1
Aldehydes	Propanal	—	1.6
	2-Methylpropanal	0.7	1.9
Ketones	2-Butanone	0.7	2.1
	3-Pentanone	—	2.3
	2-Methyl-3-pentanone	3.0	5.4
Methyl esters	Methyl formate	3.6	2.4
	Methyl acetate	10.5	9.9
	Methyl propanoate	4.6	14.0
	Methyl butanoate	1.0	2.7
	Methyl isobutanoate	4.1	13.7
	Methyl pentanoate	1.2	1.6
	Propyl acetate	2.0	1.4

[a] The GC analysis employed here could not separate 3-pentanol and 2-pentanol. However, it is evident from the synthesis patterns that 2-pentanol was absent because its corresponding ketone, 2-pentanone, was not found (or was observed only in a trace quantity) among the products while 3-pentanone appeared in quantities comparable to those of 3-pentanol. Hence, the (2-pentanol + 3-pentanol) peak was assigned to pure 3-pentanol.

bon is expressed here as a multiple of the natural abundance of ^{13}C, 1.11 atom%.

A reference ^{13}C-NMR spectrum was obtained for an alcohol mixture containing approximately equimolar quantities of methanol, ethanol, 1-propanol, and 1-butanol containing ^{13}C in its natural abundance. The spectrum is shown in Fig. 3. It is evident that each carbon in these alcohols exhibited a unique resonance and that the relative peak heights were directly related to the mole fraction of the particular carbons present. This is further demonstrated by the inserted table in Fig. 3, where the mole fractions of the alcohols were calculated from the peak heights.

Using the *0.43 mol% Cs/Cu/ZnO catalyst*, which contains the near-optimum ce-

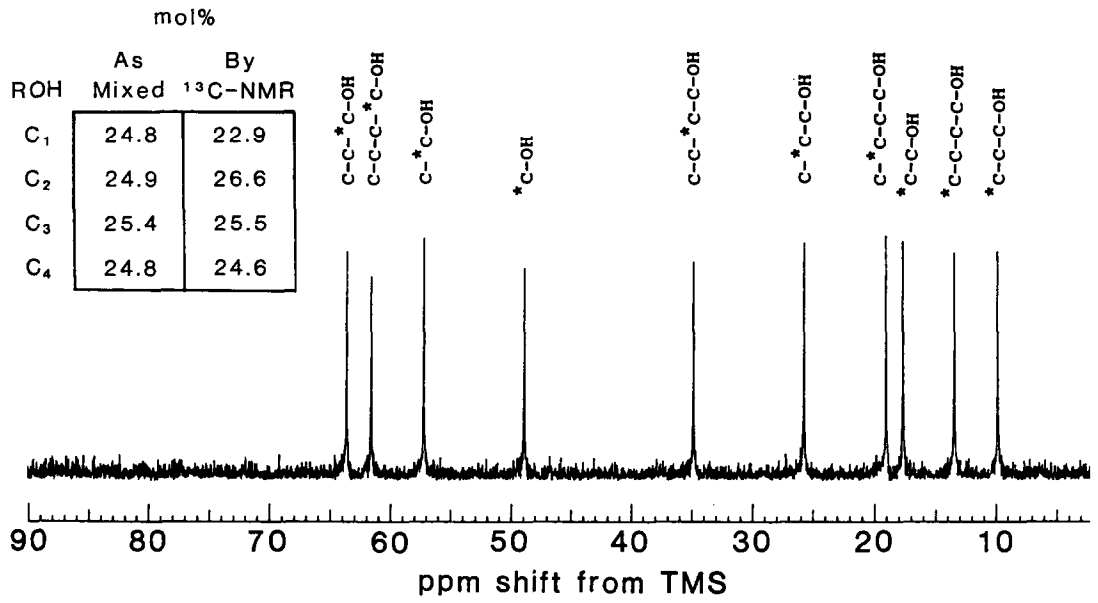

FIG. 3. ^{13}C-NMR spectrum of an approximately equimolar mixture of methanol, ethanol, 1-propanol, and 1-butanol.

sium level for the synthesis conditions utilized (Table 1), nonenriched and ^{13}C-enriched ethanol were injected in turn into the CO/H_2 reactant gas under steady-state conditions at 513, 533, 553, and 573 K. The rate of injection was 10 μl liquid ethanol/min into 133 ml synthesis gas/min, which resulted in a reactant feed of $H_2/CO/C_2H_5OH$ = 1.00/1.22/0.07 molar ratio. In each case, liquid samples were collected for analysis, and the resultant ^{13}C-NMR spectra of the products are shown in Figs. 4–7. For the reference experiments using nonenriched ethanol or methanol, it was found that the carbon mole fraction (C_x) ratio as determined by NMR and GC analyses of the product (C_x^{NMR}/C_x^{GC}) varied from 0.9 to 1.1 for the major alcohols and from 0.7 to 1.3 for the minor products. However, for the ^{13}C-NMR enrichment experiments, the low-intensity peaks were burdened by larger errors and subsequently enrichment of a given carbon was assumed to have occurred for measured ratios (enrichments) of ≥ 2.

TABLE 3

Effect of Cesium Loading of the Binary Cu/ZnO Catalyst on the Selectivity (S) for Higher Oxygenate Synthesis[a]

Catalyst	Product yield (g/kg cat/hr)		S
	Methanol	C_2^+ oxygenates	(wt%)
Undoped Cu/ZnO	204	110	35.0
0.25 mol% Cs/Cu/ZnO	181	165	47.7
0.34 mol% Cs/Cu/ZnO	157	220	58.4
0.43 mol% Cs/Cu/ZnO	162	137	45.8
1.5 mol% Cs/Cu/ZnO	213	42.8	16.7

[a] S = [C_2^+ oxygenates/(Methanol + C_2^+ Oxygenates)] × 100 in wt%. Experimental conditions are given in Table 1.

From a comparison of the natural-abundance ^{13}C and ^{13}C-enriched compounds injected or generated in the $CH_3{}^{13}CH_2OH$ injection experiments at 513 K (Fig. 4), it is evident that scrambling of the label between the two carbons of ethanol did not occur since the ratio of the peak height for the C-1 carbon at 57.4 ppm to that for the C-2 carbon at 17.6 ppm was close to the value given by the ^{13}C-1 enrichment used. Enrichment of the 1-propanol carbons was clearly observed upon injection of enriched etha-

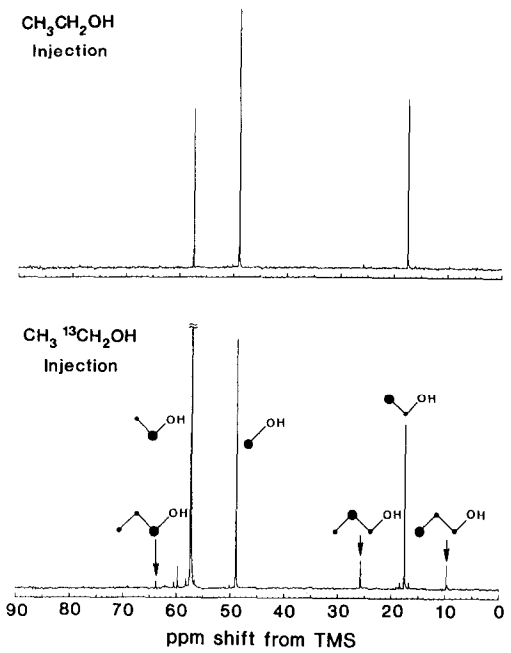

FIG. 4. Effect of injecting nonenriched ethanol and ^{13}C-1-enriched ethanol at the rate of 10 μl/min into the $H_2/CO = 0.45$ synthesis gas feed [GHSV = 3260 liters (STP)/kg cat/hr under steady-state conditions at 513 K and 7.6 MPa] on the ^{13}C-NMR spectra of the liquid product obtained over the 2.45 g of the nominal 0.4 mol% Cs/Cu/ZnO catalyst. The peaks at 59.8 ppm and 60.5 ppm are due to $HCOO\overset{\star}{C}H_2CH_3$ and $CH_3COO\overset{\star}{C}H_2CH_3$, respectively. Heavy closed circles indicate the carbon atoms associated with the observed resonances.

nol. Figures 5–7 demonstrate that the increase in reaction temperature led to the formation of higher-molecular-weight alcohols. These figures also demonstrate that the ^{13}C-enriched ethanol was being incorporated into the higher alcohols. Moreover, the ^{13}C label was observed to be located at only certain carbon positions. For example, ^{13}C enrichment in the synthesized 1-propanol was found for the C-2 (25.8 ppm) and C-3 (9.8 ppm) carbons, but no enrichment of the C-1 (63.8 ppm) carbon was observed. At low temperatures, the C-2 and C-3 carbons were equally enriched, but at the higher temperatures used, preferential enrichment at the C-3 position was observed. Thus, at temperatures above 533 K the mechanistic pathway being followed in the synthesis of 1-propanol resulted in the C-1 carbon of ethanol being preferentially incorporated as the C-3 carbon of 1-propanol, i.e.,

$$C—\overset{\star}{C}—OH \rightarrow \overset{\star}{C}—C—C—OH \quad \text{at } T > 533 \text{ K.} \quad (1)$$

For 1-butanol, the C-1 (61.8 ppm) and C-3 (19.1 ppm) carbons were preferentially enriched, i.e.,

$$C—\overset{\star}{C}—OH \rightarrow C—\overset{\star}{C}—C—\overset{\star}{C}—OH, \quad (2)$$

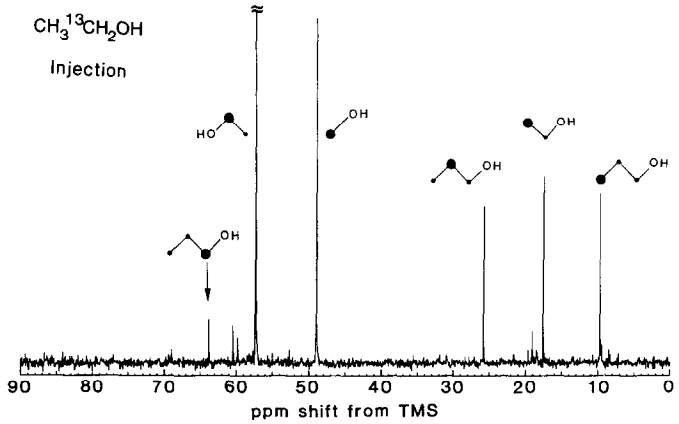

FIG. 5. ^{13}C-NMR spectrum of the liquid product obtained upon injecting ^{13}C-1-enriched ethanol into the synthesis gas feed over the 0.43 mol% Cs/Cu/ZnO catalyst at 533 K. Experimental conditions are given in Fig. 4.

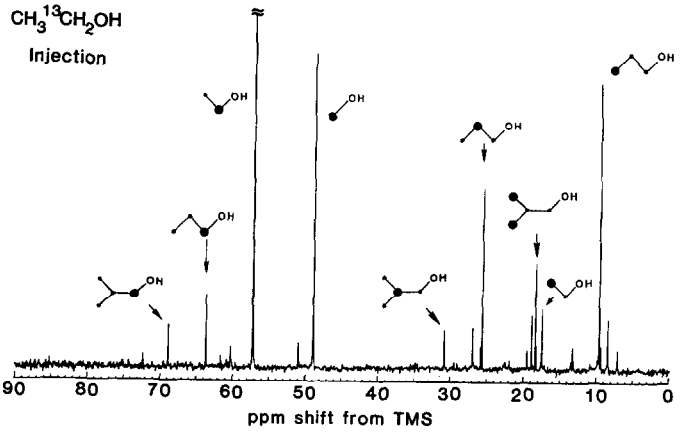

FIG. 6. ^{13}C-NMR spectrum of the liquid product upon injecting ^{13}C-1-enriched ethanol into the synthesis gas feed over the 0.43 mol% Cs/Cu/ZnO catalyst at 553 K. Experimental conditions are given in Fig. 4.

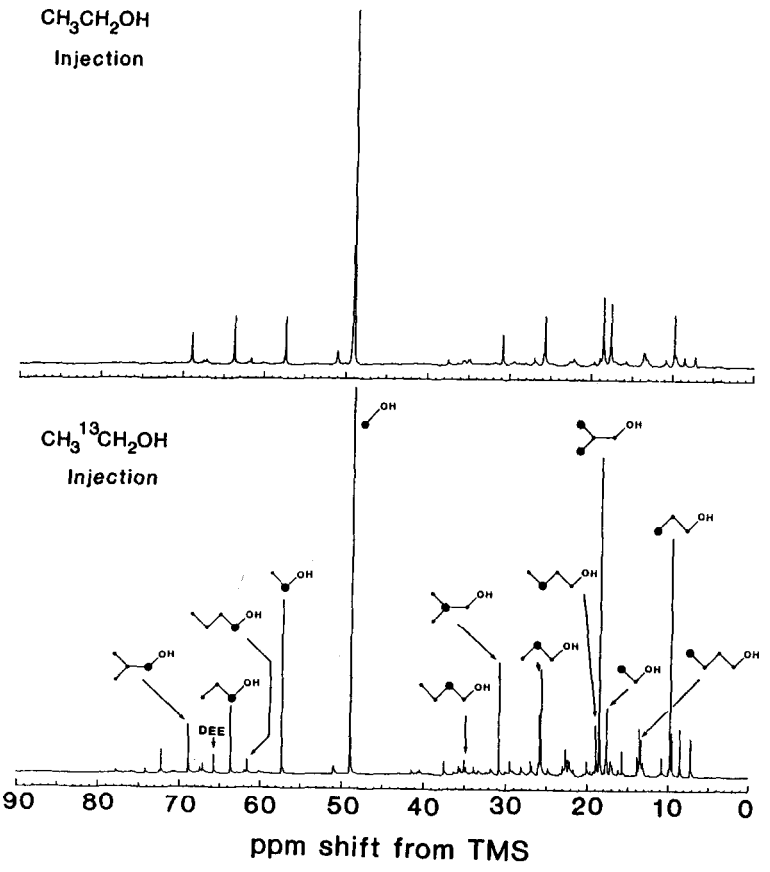

FIG. 7. Effect of injecting nonenriched ethanol and ^{13}C-1-enriched ethanol into the synthesis gas feed over the 0.43 mol% Cs/Cu/ZnO catalyst at 573 K on the ^{13}C-NMR spectra of the liquid product. Experimental conditions are given in Fig. 4.

TABLE 4

Effect of Injection of Ethanol[a] into the H_2/CO = 0.45 Synthesis Gas Stream at 7.6 MPa and GHSV = 3260 Liters (STP)/kg cat/hr on the Yield of Products Formed over a 0.4 mol% Cs/Cu/ZnO Catalyst

Product	Product yields (g/kg cat/hr)							
	T = 513 K		T = 533 K		T = 553 K		T = 573 K	
	No ethanol injection	With ethanol injection	No ethanol injection	With ethanol injection	No ethanol injection	With ethanol injection	No ethanol injection	With ethanol injection
Methanol	133	172	232	293	266	248	171	160
Ethanol	0.9	145	3.3	117	12.6	66	19	29
Methyl acetate	0.14	5.7	0.4	18.7	5.0	41	8	11
1-Propanol	—	5.7	1.1	20.5	7.4	52	19	44
2-Methyl-1-propanol	—	—	—	1.0	1.3	18.6	16.9	42.7
1-Butanol	—	1.2	—	2.4	1.8	11.3	4.9	10.7
2-Butanol	—	—	—	3.8	—	3.9	0.8	4.9
2-Butanone	—	—	—	—	—	1.9	—	3.0
2-Methyl-1-butanol	—	—	—	—	—	4.5	—	6.8

[a] Ethanol was injected at the rate of 193 g/kg cat/hr.

while the C-2 (31.0 ppm) and the terminal (18.6 ppm) carbons of 2-methyl-1-propanol were the points of enrichment for this branched alcohol. It was further observed that at low temperatures, enrichment of the C-2 carbon of 2-methyl-1-propanol dominated, whereas at high temperatures enrichment of the terminal $-CH_3$ groups dominated. These observations are consistent with aldol condensation of the C-3-enriched 1-propanol with the C_1 intermediate as discussed in Section B of the Discussion.

In the case of ethanol resonances, the ratio R_{12} of ^{13}C in the C-1 and C-2 carbons, where the C-2 carbon was not enriched, was always substantially greater than one, and this indicated that even at 573 K scrambling of the label had not occurred. The observed decrease in the ratio R_{12} with increasing temperature is undoubtedly due to dilution of the injected ethanol by nonenriched ethanol synthesized over the catalyst from CO/H_2. The effects of injection of enriched ethanol on the yields of the principal oxygenates are shown in Table 4. It can be seen that ethanol injection resulted in moderate changes in the methanol yields, but in very large increases in the yields of the higher oxygenates. Thus, at 533 K the injection of ethanol caused the formation of nearly all of the 1-butanol, 2-butanol, and 2-methyl-1-propanol observed in the product, and it increased the yields of 1-propanol by a factor of 18.6 and of methyl acetate by a factor of 47. These results clearly substantiate the conclusion that ethanol is the major carbon source for the synthesis of C_3^+ oxygenates.

To exploit the [^{13}C]ethanol injection experiments to the fullest, ^{13}C enrichment factors were calculated for all of the individual carbons of the product mixture. The method employed was similar to that previously described (*2*), except that in the present case the nonenriched C-2 carbon of ethanol was used as an internal standard. The results for the C_1–C_5 alcohols are presented in Table 5. The calculated enrichment factors are in agreement with the qualitative conclusions drawn from comparisons of the NMR spectra in Figs. 4–7.

Identical sets of the reference and ^{13}C-1-enriched ethanol injection experiments were performed over the *undoped binary Cu/ZnO catalyst* at the same four reaction temperatures (513, 533, 553, and 573 K) used with the Cs/Cu/ZnO catalyst. ^{13}C-NMR spectra for the 533 and 573 K experiments are compared in Figs. 8 and 9 and the calculated enrichment factors are summarized in Table 6. From Table 6 and Figs. 8 and 9, it is evident that only the C-2 carbons

TABLE 5

^{13}C Enrichment Factors for Each Carbon, Relative to the Ethanol C-2 Carbon, of the Alcohols Formed over the 0.4 mol% Cs/Cu/ZnO Catalyst upon Injection of $CH_3{}^{13}CH_2OH$[a]

Product alcohol	^{13}C enrichment factor			
	T = 513 K	T = 533 K	T = 553 K	T = 573 K
CH_3OH	0.9	1.0	0.9	0.7
CH_3 | CH_2OH	1.0 10.9	1.0 14.7	1.0 8.6	1.0 2.4
CH_3 | CH_2 | CH_2OH	5.5 6.4 2.3	9.8 6.3 1.8	6.5 3.7 1.6	3.1 1.4 0.9
$(CH_3)_2$[b] | CH_2 | CH_2OH	 — 	9.2 7.9 —	6.8 3.9 —	5.0 1.8 0.6
CH_3 | CH_2 | CH_2 | CH_2OH	 	2.9 12.3 ND[c] 6.4	2.9 5.8 1.2 1.8	2.5 3.3 0.8 1.1
CH_3 | $CHOH$ | CH_2 | CH_3	 	0.9 7.5 0.9 4.9	2.9 16.6 3.3 13.2	1.4 8.9 1.7 8.5
CH_3 | CH_2 | $CH(CH_3)$ | CH_2OH	 	 ND 	1.3 8.3 3.3 (3.3) 2.2	1.5 4.9 1.1 (1.9) 0.8

[a] The data used to calculate these factors were derived from the NMR spectra shown in Figs. 4–7. Ethanol was injected at the rate of 193 g/kg cat/hr.

[b] For the special case of 2-methyl-1-propanol both terminal methyl groups are equivalent; however, only one can be enriched via the aldol mechanism. Therefore, the observed enrichment was taken as a true measure of the relative rate leading to enrichment of this carbon, and no correction for the presence of two equivalent carbons was necessary.

[c] Not detected.

of 1-propanol and 2-methyl-1-propanol were enriched, i.e.,

$$C—\overset{\star}{C}—OH \rightarrow C—\overset{\star}{C}—C—OH \quad (3)$$

and

$$C—\overset{\star}{C}—OH \rightarrow C—\overset{\star}{C}—C—OH \rightarrow \begin{matrix} & & C & \\ & \diagdown & & \\ & & \overset{\star}{C}—C—OH. & \\ & \diagup & & \\ & & C & \end{matrix} \quad (4)$$

Thus, it is clear that there are distinct differences in the reaction pathways of higher alcohol synthesis over the Cs-doped and the undoped Cu/ZnO catalysts. Analogous to the observations with the Cs/Cu/ZnO catalyst, the addition of ethanol to the reactant CO/H_2 stream led to a dramatic increase in the synthesis of C_3^+ oxygenates, again supporting the conclusion that ethanol was a direct precursor in the formation of the higher-molecular-weight oxygenates.

As already noted, the reaction product also contained small quantities of methyl esters of the carboxylic acids correspond-

TABLE 6

^{13}C Enrichment Factors for Each Carbon, Relative to the Ethanol C-2 Carbon, of the Alcohols Formed over the Undoped Cu/ZnO Catalyst upon Injection of $CH_3{}^{13}CH_2OH$[a]

Product alcohol	^{13}C enrichment factor			
	T = 513 K	T = 533 K	T = 553 K	T = 573 K
CH_3OH	0.7	0.8	0.8	0.7
CH_3 | CH_2OH	1.0 13.4	1.0 17.2	1.0 11.2	1.0 3.8
CH_3 | CH_2 | CH_2OH	1.5 12.1 2.5	1.3 15.6 1.5	1.6 8.4 1.3	1.1 2.5 0.8
$(CH_3)_2$[b] | CH_2 | CH_2OH	 ND[c] 	— 5.6 —	3.2 8.9 —	3.8 6.2 —
CH_3 | CH_2 | CH_2 | CH_2OH	 	0.9 13.6 1.7 5.2	1.3 9.3 0.9 2.5	1.1 4.6 0.8 1.4
CH_3 | $CHOH$ | CH_2 | CH_3	— 4.9 1.9 4.0	0.6 4.1 1.3 3.2	1.0 4.7 1.1 2.7	1.5 4.4 1.3 3.4
CH_3 | CH_2 | $CH(CH_3)$ | CH_2OH	 	 ND 	1.4 17.4 6.0 (2.4) 4.1	0.8 5.3 1.5 (1.8) 0.7

[a] Ethanol was injected at the rate of 193 g/kg cat/hr.

[b] As in Table 5.

[c] Not detected.

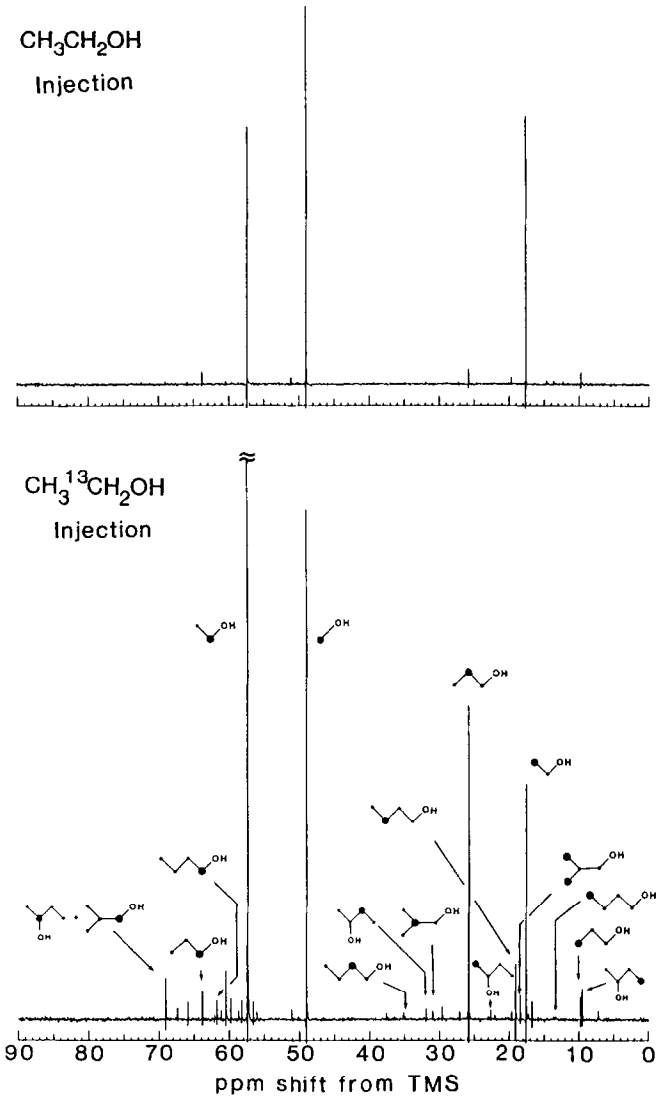

FIG. 8. Effect of injecting nonenriched ethanol and ^{13}C-1-enriched ethanol into the synthesis gas feed over the nonpromoted Cu/ZnO catalyst at 533 K on the ^{13}C-NMR spectra of the liquid product. Experimental conditions are given in Fig. 4.

ing to the principal alcohols, as well as the corresponding aldehydes and ketones. The aldehydes and most of the methyl esters were not detected in sufficient quantities that would allow reliable ^{13}C enrichment factors to be calculated from the observed ^{13}C-NMR spectra. However, at 553 K with both the undoped and the Cs-promoted catalysts, the ^{13}C-NMR spectra of 2-butanone and methyl propanoate were sufficiently resolved so that the enrichment factors could be calculated for all of the carbons except the carbonyl carbon. The results for these two products are presented in Table 7 and are compared with the enrichment factors obtained for the expected parent alcohols. Clearly, the acyl fragment of the ester was derived from the corresponding alcohol.

To complement the deductions made from the labeled ethanol injection experiments, a set of experiments was carried out in which a $^{13}CH_3OH/^{12}CH_3{}^{12}CH_2OH$ etha-

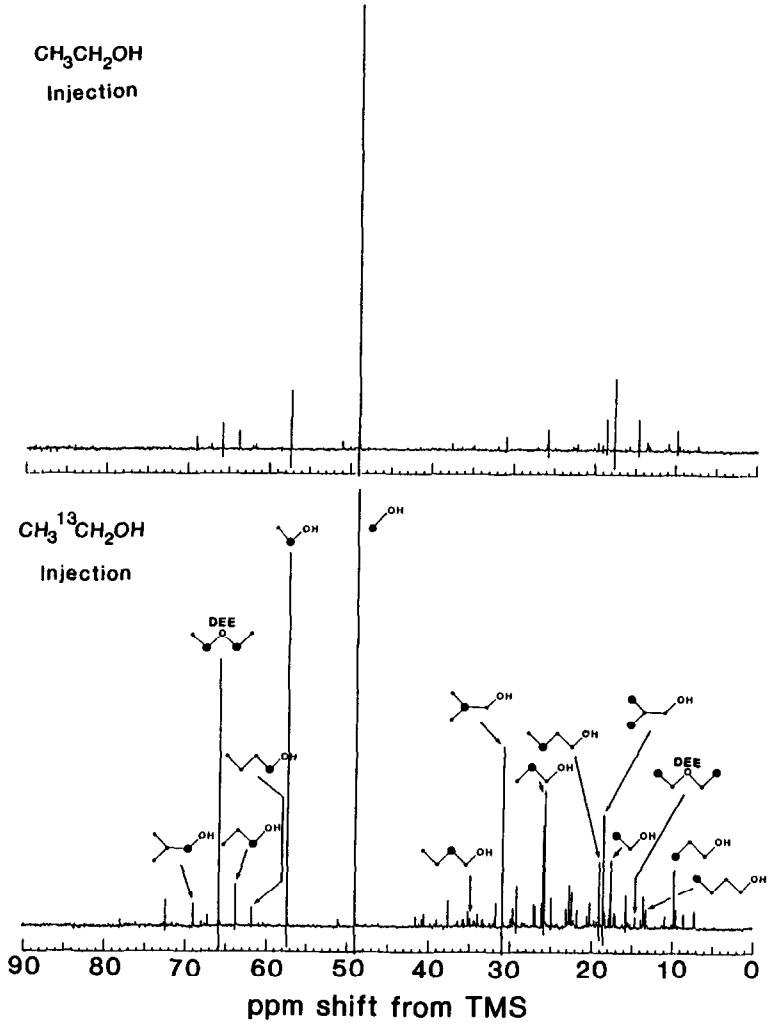

FIG. 9. Effect of injecting nonenriched ethanol and ^{13}C-1-enriched ethanol into the synthesis gas feed over the nonpromoted Cu/ZnO catalyst at 573 K on the ^{13}C-NMR spectra of the liquid product. Experimental conditions are given in Fig. 4.

nol mixture was injected into the synthesis gas stream over both the undoped Cu/ZnO catalyst and the 0.4 mol% Cs/Cu/ZnO catalyst. The ^{13}C-NMR spectra of the liquid products for these experiments at 533 K are presented in Figs. 10 and 11. Over the undoped catalyst (Fig. 10), the C-1 carbon of the synthesized 1-propanol had been selectively enriched and the carbon of the methoxy group of methyl acetate was greatly enriched in comparison with the other carbons, i.e.,

$$C—C—OH + \overset{\star}{C}—OH \rightarrow C—C—\overset{\star}{C}—OH \quad (5)$$

$$C—\overset{O}{\overset{\|}{C}}—H + \overset{\star}{C}—OH \rightarrow C—\overset{O}{\overset{\|}{C}}—O—\overset{\star}{C}. \quad (6)$$

Similar results characterized by Eqs. (5) and (6) were obtained with the 0.4 mol% Cs/Cu/ZnO catalyst, as shown in Fig. 11.

Enrichment factors were calculated for both sets of experiments using unlabeled

TABLE 7

Comparisons of the ^{13}C Enrichment Factors for 1-Propanol, Methyl Propionate, 2-Butanol, and 2-Butanone Formed over Cu/ZnO and Cs-Promoted Cu/ZnO Catalysts at 553 K upon Injection of $CH_3{}^{13}CH_2OH$[a]

Product	^{13}C enrichment factor	
	Undoped Cu/ZnO	0.4 mol% Cs/Cu/ZnO
CH_3	1.6	6.5
CH_2	8.4	3.7
CH_2OH	1.3	1.4
CH_3	1.3	4.6
CH_2	7.4	2.4
$C{=}O$	—	—
O		
CH_3	1.3	0.6
CH_3	1.0	2.9
CHOH	4.7	16.6
CH_2	1.1	3.3
CH_3	2.7	13.2
CH_3	1.0	1.1
$C{=}O$	—	—
CH_2	1.5	3.5
CH_3	5.1	12.7

[a] Ethanol was injected at the rate of 193 g/kg cat/hr.

ethanol as an internal standard and by combining the observed ^{13}C-NMR spectra data with product mole fractions determined by GC analyses. These enrichment factors are presented in Tables 8 and 9 for the Cu/ZnO and the 0.4 mol% Cs/Cu/ZnO catalysts, respectively. For the $^{13}CH_3OH/^{12}CH_3{}^{12}CH_2OH$ ethanol injection experiments, the calculated enrichment factors again clearly show that the C-1 carbon of 1-propanol and the methoxy carbon of methyl acetate were preferentially enriched. The two carbons of ethanol have also been somewhat enriched in the $^{13}CH_3OH$/1-propanol injection experiment due to synthesis of ethanol from methanol as previously shown (*2*). At the higher reaction temperatures of 533 and 553 K, enrichments occurred over both catalysts in the C-1 carbon of 1-propanol, C-1 and C-2 carbons of 1-butanol, and C-1 and C-3 carbons of 2-methyl-1-propanol, i.e.,

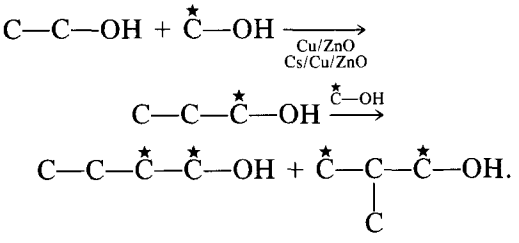

(7)

This is further supported by the observed enrichment factors obtained in the $^{13}CH_3OH/^{12}CH_3{}^{12}CH_2{}^{12}CH_2OH$ propanol injection experiments (Table 10), i.e.,

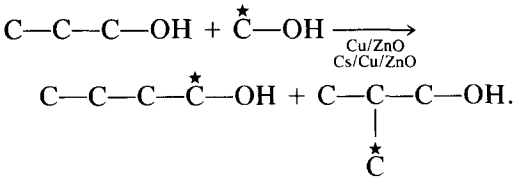

(8)

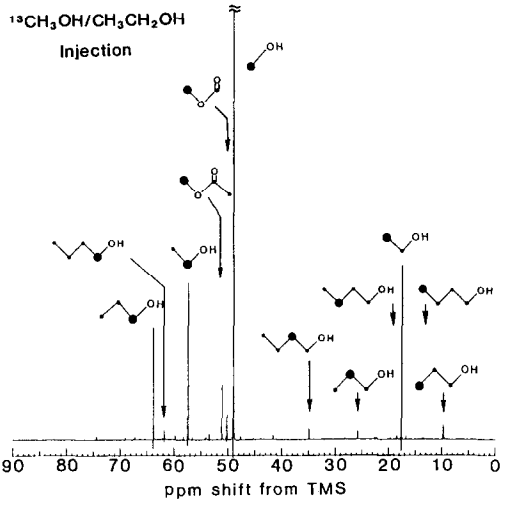

FIG. 10. ^{13}C-NMR spectrum of the liquid product obtained upon injection of a [^{13}C]methanol/ethanol = 1 : 32 mixture at the rate of 10 μl/min into the H_2/CO = 0.45 synthesis gas feed [GHSV = 3260 liters (STP)/kg cat/hr under steady-state conditions at 533 K and 7.6 MPa] over the undoped Cu/ZnO catalyst. The ^{13}C enrichment of methanol was 90.1.

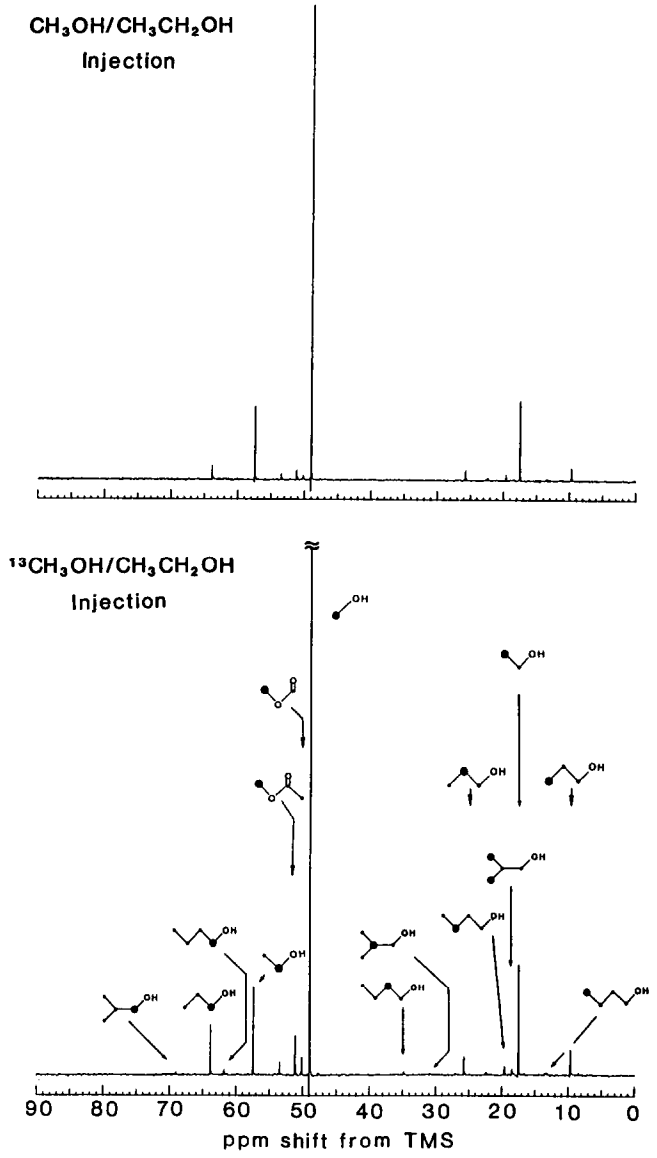

FIG. 11. Effect of injecting a nonenriched methanol/ethanol mixture and a ^{13}C-labeled methanol/ethanol mixture into the synthesis gas feed over the 0.4 mol% Cs/Cu/ZnO catalyst at 533 K on the ^{13}C-NMR spectra of the liquid product. Experimental conditions are given in Fig. 10.

Thus, the active C_1 intermediate giving rise to the methyl group of the methyl esters and to linear chain growth in high alcohol synthesis was preferentially derived from gas-phase methanol rather than from CO. This is further supported by the observation that with the Cs/Cu/ZnO catalyst at 573 K, no enrichment of the carbons in the alcohol products was observed upon injection of $^{13}CH_3OH/^{12}CH_3{}^{12}CH_2OH$ (Table 9). This arose because methanol at this temperature was in equilibrium with CO and H_2, and thus the ^{13}C of the injected methanol was effectively lost by dilution by the much

TABLE 8

^{13}C Enrichment Factors for the Principal Products Formed over Undoped Cu/ZnO Catalyst upon Injection of a $^{13}CH_3OH/CH_3CH_2OH$[a] Mixture into the $H_2/CO = 0.45$ Synthesis Gas

Product	^{13}C enrichment factor			
	$T = 513$ K	$T = 533$ K	$T = 553$ K	$T = 573$ K
CH_3OH	17.4	8.4	2.1	1.0
CH_3 | CH_2OH	1.0	1.0	1.0	1.0
CH_3 | CH_2 | CH_2OH	1.3 0.8 10.3	1.6 1.0 11.3	1.2 1.0 3.4	0.9 0.7 1.2
CH_3 | O | C=O | CH_3	5.5 — 1.0	5.9 — 1.0	1.3 — 0.5	0.7 — 0.7
CH_3 | CH_2 | CH_2 | CH_2OH	 	1.3 1.0 7.3 6.3	1.0 1.0 2.7 2.1	1.2 1.0 1.8 1.2
$(CH_3)_2$[b] | CH_2 | CH_2OH	 	 	5.8 0.8 4.7	5.8 1.3 2.1
CH_3 | CH_2 | $CH(CH_3)$ | CH_2OH	 	 	0.8 0.6 2.3 (1.7) 2.9	0.9 0.9 1.2 (1.3) 1.2

[a] Simultaneous injection of methanol (47 g/kg cat/hr) and ethanol (147 g/kg cat/hr).
[b] As in Table 5.

more abundant carbon of the CO reactant in the synthesis gas feed.

DISCUSSION

A. *Effect of Cesium Doping on Reaction Rate and Selectivity*

From the results presented in Tables 1–3, it is evident that doping the Cu/ZnO catalysts with cesium promoted formation of all higher alcohols and esters with the exception of ethanol and methyl acetate. In addition, the *ratios* of the yields of branched products $RCH(CH_3)CH_2OH$ that result from β branching to those of the parent linear alcohols RCH_2CH_2OH, e.g., 2-methyl-1-propanol/1-propanol and 2-methyl-1-butanol/1-butanol, were not greatly affected by cesium loading, but there was a very marked effect on the ratio of the higher alcohols to ethanol. The ratio of 1-propanol to ethanol increased by a factor of 5 in going from the undoped to the 0.34 mol% Cs-doped Cu/ZnO catalyst, with little change in the ratio of the i-C_{n+1}/1-C_n products. Because the cesium dopant increased the *overall yield* of the C_2^+ alcohols, as well as

TABLE 9

^{13}C Enrichment Factors for the Principal Products Formed over a 0.4 mol% Cs/Cu/ZnO Catalyst upon Injection of a $^{13}CH_3OH/CH_3CH_2OH$[a] Mixture into the $H_2/CO = 0.45$ Synthesis Gas

Product	^{13}C enrichment factor			
	$T = 513$ K	$T = 533$ K	$T = 553$ K	$T = 573$ K
CH_3OH	5.9	1.7	1.0	1.1
CH_3 | CH_2OH	1.0	1.0	1.0	1.0
CH_3 | CH_2 | CH_2OH	1.0 0.7 2.3	0.8 1.0 2.6	1.3 0.7 1.5	1.0 1.0 0.7
CH_3 | O | C=O | CH_3	3.3 — 1.0	2.1 — 1.0	0.9 — 0.9	1.0 — 0.9
CH_3 | CH_2 | CH_2 | CH_2OH	 	0.7 — 1.3 1.5	1.0 0.8 1.3 1.4	1.2 1.0 1.1 0.8
$(CH_3)_2$[b] | CH_2 | CH_2OH	 	8.8 2.7 6.3	3.6 1.0 1.9	3.2 1.1 0.9
CH_3 | CH_2 | $CH(CH_3)$ | CH_2OH	 	 	1.5 1.3 1.8 (1.5) 1.7	1.1 0.7 1.1 (0.8) 0.7

[a] Simultaneous injection of methanol (47 g/kg cat/hr) and ethanol (147 g/kg cat/hr).
[b] As in Table 5.

TABLE 10

^{13}C Enrichment Factors for Products Formed over a 0.4 mol% Cs/Cu/ZnO Catalyst upon Injection of a $^{13}CH_3OH$/1-Propanol[a] Mixture into the H_2/CO = 0.45 Synthesis Gas

Product	^{13}C enrichment factor			
	T = 513 K	T = 533 K	T = 553 K	T = 573 K
CH_3OH	9.6	4.3	1.2	0.9
CH_3 | CH_2OH	2.5	5.9	2.0	1.1
CH_3 | CH_2 | CH_2OH	1.0 1.0 0.9	1.0 1.0 1.1	1.0 1.1 0.9	1.0 1.1 1.0
CH_3 | CH_2 | CH_2 | CH_2OH	— — — 15.6	2.2 1.9 1.9 8.1	1.7 1.4 1.0 2.8	0.9 1.2 1.1 1.2
$(CH_3)_2$[b] | CH_2 | CH_2OH	2.6 0.6 1.4	8.6 1.3 5.5	3.8 1.1 2.5	2.8 0.9 1.4
CH_3 | CH_2 | $CH(CH_3)$ | CH_2OH			— — — (2.5) 1.8	0.9 0.4 0.7 (1.3) 0.6

[a] Simultaneous injection of methanol (47 g/kg cat/hr) and 1-propanol (150 g/kg cat/hr).
[b] As in Table 5.

the 1-propanol/ethanol ratio, the greatest effects of cesium appear to be an increase in the ethanol synthesis rate and an even greater enhancement in the rate of ethanol conversion to 1-propanol and subsequently to higher alcohols. This explains the higher yields of C_3^+ oxygenates, accompanied by the decrease in selectivity for ethanol upon cesium promotion.

The effect of cesium loading on the overall activity of the Cu/ZnO catalyst, which consists of the rate of CO conversion passing through a dramatic maximum as a function of cesium concentration, can be attributed to the bifunctional nature of these alcohol synthesis catalysts (*6, 28*). One function is the hydrogenation function of the Cu/ZnO portion of the catalyst and the second function provided by the alkali ion and its counterion is that of a base that executes various C–C and C–O bond-forming reactions. Inhibition of alcohol synthesis occurs at high cesium loadings because above a certain surface concentration, cesium blocks the hydrogenation sites of the catalyst. The cesium doping also suppressed the production of hydrocarbons (Tables 1 and 2).

B. Mechanism of Higher Alcohol and Oxygenate Synthesis

The present ^{13}C incorporation study resulted in determination of the principal carbon source for each carbon of the product, and of the location of carbon atoms in the product molecules originating from the CO/H_2 synthesis gas and injected precursor compounds in each individual step.

The injected labeled alcohols and their mixtures were $^{12}CH_3{}^{13}CH_2OH$ ethanol, $^{12}CH_3{}^{12}CH_2OH/{}^{13}CH_3OH$ ethanol/methanol mixture, and $^{12}C_3H_7OH/{}^{13}CH_3OH$ 1-propanol/methanol mixture. Injection of the C_2 or $C_2 + C_1$ alcohols greatly enhanced the yields of C_3^+ products (Table 4), and injection of the $C_3 + C_1$ alcohol mixture greatly enhanced the yields of the C_4^+ products, demonstrating that the injected alcohols were incorporated into the synthesis very effectively. Although the C_2 and C_3 alcohols were injected in excess to their natively synthesized counterparts (Tables 5–10), their rapid incorporation permits the conclusion that the native synthesis proceeds by the same mechanism as that revealed by the isotope flow from the excess injected alcohols. The isotope flow also provides evidence of the stepwise nature of the synthesis; the major mechanistic step was a C_1 addition to a C_n precursor and the minor mechanistic step was a C_m (m = 2, 3) addition to a C_n ($n \geq 2$) precursor. The individual steps, however, still proceed via intermediates the structures of which have not been or perhaps cannot be determined. We shall nevertheless attempt to identify

such intermediates from the general knowledge of chemistry with the perspective that their identity and pathways can be verified by quantum chemical calculations when such calculations produce reliable results for the relatively large molecules involved beyond the $C_1 \rightarrow C_2$ step. MNDO calculations published earlier (*2*) led to the conclusion that the insertion of CO into alkoxide, $RO^{\ominus} + CO \rightarrow RCOO^{\ominus}$ ($R \neq H$), which had been considered as a possible linear chain growth step in alcohol synthesis (*5, 6*), is rendered unlikely by a high activation barrier, although the analogous formate-generating reaction (R = H) proceeds readily (*2*). Also, for the $C_1 \rightarrow C_2$ step, the CO insertion into methoxide must be discarded based on earlier reported ^{13}C isotope experiments (*2*). Therefore, other linear growth mechanisms have to be considered, and those that are admissible based on the outcome of the present ^{13}C labeling experiments are discussed below.

Based on the product distribution described in detail under Results, the effect of cesium on rates and selectivities, the incorporation of lower alcohols into higher alcohols, and the ^{13}C isotope distribution in the higher oxygenates upon injection of ^{13}C-enriched lower alcohols, a general reaction network can be proposed for the synthesis of higher oxygenates over the Cs-promoted Cu/ZnO catalyst. The network is essentially an extension and modification of previous reaction networks for higher oxygenate synthesis proposed by Vedage *et al.* (*6*) and by Smith and Anderson (*29*). The individual steps of the present reaction network can be grouped into several distinct reaction types:

1. *Linear chain growth* (ℓ) via C_1 addition steps at the alcohol end of the growing chain to give linear primary alcohols such as ethanol, 1-propanol, 1-butanol, etc.

2. *β addition* (β_1) between C_1 and C_n ($n \geq 2$) surface species, which results in 1-propanol ($n = 2$) and branched primary alcohols such as 2-methyl-1-propanol and 2-methyl-1-butanol ($n \geq 3$).

3. *β addition* (β_m) between C_m ($m = 2, 3$) and C_n ($n \geq 2$) surface species, which results in a variety of alcohols such as 1-butanol, 2-butanol, 1-pentanol, 2-methyl-1-butanol, 3-pentanol, 3-methyl-2-butanol, and 2-methyl-3-pentanol.

4. *Tischenko/Cannizzaro reaction* leading to methyl esters of carboxylic acids corresponding to all the synthesized alcohols.

5. *Methyl formate formation via carbonylation of methanol* as reported earlier (*2*).

Next, each of these reaction types is discussed in the light of our experimental results.

1. Stepwise linear carbon chain growth (ℓ). Two possible reaction mechanisms leading to linear chain growth that are consistent with the experimental observations can be proposed, both based on the hydrogenation-base bifunctionality of the catalyst. An adsorbed formyl species is common to both pathways as proposed earlier (*2*).

The first mechanism involves the nucleophilic attack at the α carbon of an adsorbed aldehydic intermediate by formyl $HCO^{\ominus}$, yielding a dioxygenated species. This species subsequently undergoes hydrogenation/dehydration to yield the C_{n+1} alcohol. As postulated originally by Fox *et al.* (*14*) and adopted by the authors in the preceding paper (*2*), formaldehyde as the adsorbed aldehydic intermediate upon nucleophilic attack by the formyl generates the C_2 precursor of ethanol. A second similar mechanism involves the nucleophilic attack by the formyl species of the C-1 position of an adsorbed alcohol, with its hydroxyl being the leaving group, or an analogous acyl-methanol reaction. The displacement of the hydroxyl would thus occur by an S_N2 mechanism. Based on either of the above outlined linear growth mechanisms, it can be rationalized why, in the case of the $^{12}CH_3$ $^{13}CH_2OH$ ethanol injection experiments, the ^{13}C label can be found at the C-2 carbon of 1-propanol (cf. Tables 5 and 6). In addition, direct identification of the source of the active C_1 surface species as a derivative

of methanol was confirmed upon injection of $^{13}CH_3OH/^{12}CH_3{}^{12}CH_2OH$ ethanol mixtures that gave rise to 1-propanol enriched at the C-1 carbon. The subsequent enrichment of the C-1 and C-2 carbons of 1-butanol was also observed (cf. Tables 8 and 9).

Unique to the observed higher-molecular-weight production distribution is the absence of observable yields of such reaction products as 3-methyl-1-butanol and 3-methyl-1-pentanol that would result from the linear chain growth of 2-methyl-1-propanol and 2-methyl-1-butanol. The absence of these products can be explained by electronic and steric restrictions of the two linear chain growth steps discussed above. The adsorbed aldehydic derivative of the branched alcohols may be rendered less susceptible to nucleophilic attack by the inductive effect of alkyl substituents at the β carbon position. In regard to the steric factor, the rates would decrease as the size of the substituent on the C-1 carbon of the alcohol increases, the occurrence of β branching inhibiting the linear pathway of chain growth (*30*).

2. β additions involving the $C_n + C_1$ ($n \geq 2$) and the $C_n + C_m$ ($n, m = 2, 3$) steps. The product composition presented in Table 2 and the patterns of ^{13}C incorporation into the specific carbons of the product molecules from various ^{13}C-labeled precursor alcohols presented in Tables 5–10 demonstrate the significance of reactions at the β carbon of the growing oxygenate chain,

$$\begin{matrix} -C-C-C-O \\ \gamma\ \ \beta\ \ \alpha \end{matrix} .$$

The attack on the β carbon by the C_1 intermediate dominates in the synthesis, but additional minor paths associated with the attack of β carbon by C_m ($m = 2, 3$) intermediates are also operating. The cesium promoter enhances the rates of all $C_n \rightarrow C_n^+$ ($n \geq 2$) synthetic steps but particularly of the $C_2 \rightarrow C_3$ step. As the cesium counterions are basic, the whole reaction pattern will be discussed in terms of base-catalyzed β additions. Because of the prominence and facile course of these β additions in aldehyde and ketone chemistry, it will be assumed that the reactive species in the present system are enolates, or carbanions, that are formed from the precursor alcohols by dehydrogenation and ionization in the vicinity of the surface cesium ions.

A general scheme involving aldehydes which accounts for all the products and ^{13}C distribution patterns is Scheme I.

The β-ketoalkoxide that is formed by the condensation of an RR′ enolate with an R″ aldehyde (R″ = H for C_1 addition) further undergoes isomerization, hydrogenation, hydrolytic, and dehydration reactions **1–3** (Scheme II), the relative rates of which determine the relative abundance of the two principal types of products, $R''CH_2CHRCHR'OH$ and $R'CH_2CHRCHR''OH$. The initial reaction, in which the two aldehydes are coordinated to the Cs^+ ion, requires that the two oxygens of the β-ketoalkoxide are in *cis* position. In addition, stereoisomerization exemplified by path **4** (Scheme III), which gives rise to conformations with distal oxygens, will occur at a rate that will depend upon the nature of substituents R and R′ and their interaction

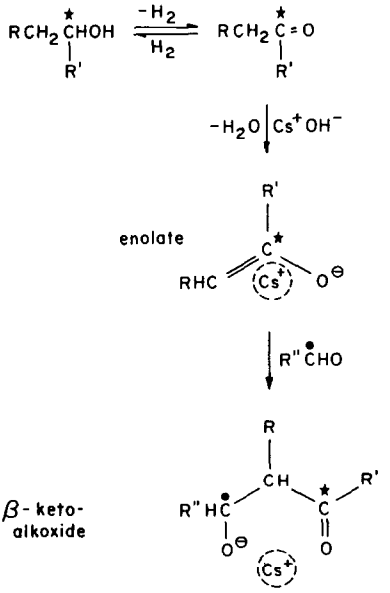

SCHEME I

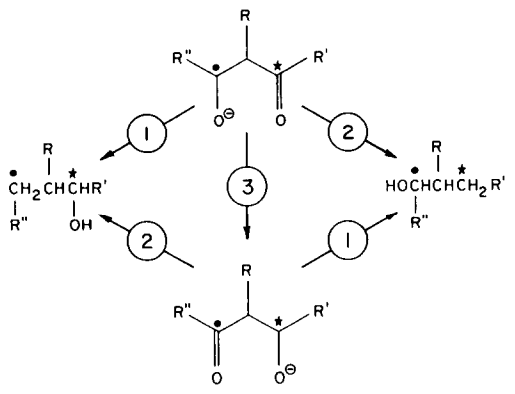

SCHEME II

with the catalyst surface. The labels ● and ★ mark carbon atoms the specific location of which can and has been revealed by the various ^{13}C-labeling experiments employed here.

Each of the paths **1–3** may occur by a sequence of partial reactions, viz.:

1 hydrolysis of the Cs^+–alkoxide bond
dehydration of the alcohol group
hydrogenation of the product;

2 hydrogenation of the carbonyl group
dehydration of the alcohol
hydrolysis of the Cs^+–alkoxide bond
hydrogenation of the product;

3 dehydrogenation of the
R″—CH—CH—R functionality to
R″—C=C—R, isomerization
$^{\ominus}OCR''=CR(CO)R' \rightarrow$
$R''(CO)CR=CR'O^{\ominus}$, hydrogenation.

As an example, we give the specific course of path **2**:

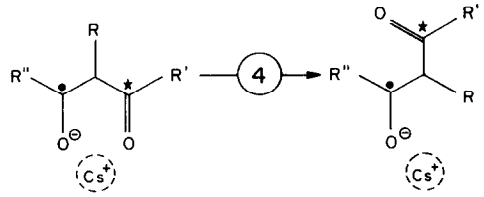

SCHEME III

$$^{\ominus}OCHR''CHRC(O)R' \xrightarrow{H_2}$$
$$^{\ominus}OCHR''CHRCHR'OH \xrightarrow{-H_2O}$$
$$^{\ominus}OCHR''CR{=}CHR' \xrightarrow[-OH^{\ominus}]{H_2O}$$
$$HCOHR''CR{=}CHR' \xrightarrow{H_2}$$
$$HOCHR''CHRCH_2R'.$$

The two alcohol products of Scheme II are listed in Table 11 in terms of the combination of substituents R, R′, and R″, injected compounds and their isotopic composition, and the paths involved.

The path labeled N gives a product that is expected in *normal* aldol synthesis followed by hydrogenation, whereas path R gives a product in which the oxygen retention is *reversed* from that expected in aldol synthesis. Path N can occur directly by sequence **1** of Scheme II or by sequence 3 followed by **2**. Path R can occur directly by sequence **2** or by sequence **3** followed by **1**. Path R will be termed here *aldol coupling with oxygen retention reversal.*

Results in Tables 5–10 demonstrate that path R is significant over both the Cs/Cu/ZnO and the Cu/ZnO catalysts and particularly dominates in the $C_2 \rightarrow C_3$ step over the Cs/Cu/ZnO catalyst at high temperatures where the product $CH_3\overset{\bullet}{C}H_2\overset{\star}{C}H_2OH$, given in parentheses, is not observed. Further, all observed products are accounted for by the paths R and N represented by Scheme II, operating with varying degrees in different $C_n \rightarrow C_n^+$ steps. The patterns that have emerged and the mechanistic implications thereof are discussed below for each individual synthetic step.

$C_2 \rightarrow C_3$ synthesis. This step, realized by a reaction of ethanol with either methanol or CO/H_2, occurs by linear growth ℓ and by β addition to given 1-propanol in both cases. Over the Cu/ZnO catalyst, the linear growth ℓ is the principal mechanism, as ethanol enriched by ^{13}C at C-1 yields mainly 1-propanol enriched at C-2, $C—\overset{\star}{C}—O + C—O \rightarrow C—\overset{\star}{C}—C—O$ (cf. Tables 6 and 7). Over the Cs/Cu/ZnO catalyst, the β addi-

TABLE 11

R	R′	R″	Injected compound	Product	Path
H	H	H	$CH_3\overset{\star}{C}H_2OH + \overset{\bullet}{C}H_3OH$	$(\overset{\bullet}{C}H_3CH_2\overset{\star}{C}H_2OH)$	N
				$\overset{\star}{C}H_3CH_2\overset{\bullet}{C}H_2OH$	R
CH_3	H	H	$CH_3CH_2CH_2OH + \overset{\bullet}{C}H_3OH$	$(\overset{\bullet}{C}H_3)_2CHCH_2OH$	N
				$(CH_3)_2CH\overset{\bullet}{C}H_2OH$	R
H	CH_3	H	$(CH_3)_2CHOH$	$CH_3CH_2CHOHCH_3$	N
				$CH_3CH_2CH_2CH_2OH$	R
H	H	CH_3	$2CH_3\overset{\star}{C}H_2OH$	$CH_3\overset{\star}{C}H_2CH_2\overset{\star}{C}H_2OH$	N
				$CH_3\overset{\star}{C}HOHCH_2\overset{\star}{C}H_3$	R
CH_3	H	CH_3	Native synthesis	$CH_3CH_2CH(CH_3)CH_2OH$	N
				$CH_3CHOHCH(CH_3)_2$	R
H	H	C_2H_5	Native synthesis	$CH_3(CH_2)_4OH$	N
				$(C_2H_5)_2CHOH$	R
CH_3	H	C_2H_5	Native synthesis	$CH_3(CH_2)_2CH(CH_3)CH_2OH$	N
				$C_2H_5(CHOH)CH(CH_3)_2$	R

tion is greatly accelerated and occurs almost exclusively by the aldol coupling with oxygen retention reversal R, as demonstrated by the outcome of C-1-enriched ethanol injection,

$$C—\overset{\star}{C}—O + C—O \rightarrow \overset{\star}{C}—C—C—O \quad (9)$$

(cf. Tables 5 and 7). This striking result is explained as follows: the *cis*-β-ketoalkoxide $^{\ominus}O\overset{\bullet}{C}H_2CH_2\overset{\star}{C}HO$, derived from $C_2 + C_1$ addition, isomerizes by **4** to a conformer in which only the alkoxy oxygen is bonded to the Cs^+ ion, while the distal carbonyl group is hydrogenated on the Cu/ZnO surface, dehydrated, hydrogenated, and hydrolytically released as $\overset{\star}{C}H_3CH_2\overset{\bullet}{C}H_2OH$. The $\overset{\star}{C}H_3CH_2-$ group originates from the labeled ethanol and the $-\overset{\bullet}{C}H_2OH$ group from the C_1 intermediate. The latter assignment has been confirmed by allowing unlabeled ethanol to react with labeled methanol, with the result (cf. Tables 8 and 9)

$$C—C—O + \overset{\bullet}{C}—O \rightarrow C—C—\overset{\bullet}{C}—O \quad (10)$$

obtained over both the Cu/ZnO and the Cs/Cu/ZnO catalysts.

The $C_2 \rightarrow C_3$ chemistry is symbolically summarized as

Cu/ZnO catalyst:

$$\ell \gg \beta(N) \approx \beta(R)$$

Cs/Cu/ZnO catalyst:

$$\ell \approx \beta(R) > \beta(N) \quad T < 530\ K$$
$$\beta(R) > \ell \gg \beta(N) \quad T > 530\ K$$

showing that the Cs dopant accelerates the $C_2 \rightarrow C_3$ conversion by greatly promoting the $C_2 + C_1$ coupling reaction with oxygen retention reversal. This, then, is the mechanistic cause for a product distribution with ethanol at minimum and C_3^+ alcohols and methanol at maximum.

$C_3 \rightarrow C_4$ synthesis. 1-Propanol yields 1-butanol, a minor product, by the linear growth ℓ and 2-methyl-1-propanol, a major product, by the β(N) and β(R) additions. The β(N) and β(R) paths are distinguished by the position of ^{13}C from labeled methanol in the 2-methyl-1-propanol product, and results presented in Table 10 for the Cs/Cu/ZnO catalyst show that the β(N) path is slightly more effective than the β(R) path at all temperatures. Injection of 2-propanol is predicted to yield 2-methyl-1-propanol by ℓ, 2-butanol by β(N), and 1-butanol by β(R). Results obtained by Young (*31*) show that ℓ is a very minor pathway for 2-pro-

panol while β(N) and β(R) occur at comparable rates, with β(R) slightly favored at high temperatures over the Cs/Cu/ZnO catalyst.

The $C_3 \rightarrow C_4$ synthetic steps are thus dominated by the β additions. The β(R) path is still kinetically significant but it is no longer strongly favored over β(N) as in the $C_2 \rightarrow C_3$ step. The key to the difference in the relative rates β(N) and β(R) for the $C_3 \rightarrow C_4$ and the $C_2 \rightarrow C_3$ steps appears to be the presence of the methyl substituents (R = CH_3 for 1-propanol and R′ = CH_3 for 2-propanol) in the $C_3 \rightarrow C_4$ steps. These substituents are suggested to frustrate path **4** by their steric interaction with the catalyst surface, thus favoring the *cis* conformation of the β-ketoalkoxide of Schemes I and II which can then undergo conversions **1, 2, 3 + 1,** and **3 + 2** to both products of the β(N) and β(R) additions. Path **4,** however, favors only the product of the β(R) addition. Because β(R) is the exclusive course of the $C_2 \rightarrow C_3$ β addition, it must be concluded that the stereoisomerization **4** is fast compared to **1, 2,** and **3** for the sterically unhindered $C_2 \rightarrow C_3$ step with R = R′ = R″ = H.

Aside from steric factors, electronic and thermodynamic factors were considered to explain the difference in the β(N)/β(R) selectivity between the $C_2 \rightarrow C_3$ and the $C_3 \rightarrow C_4$ additions. Taking into account that the methyl substituent in 1-propanol (R = CH_3) is attached to the β carbon while that in 2-propanol (R′ = CH_3) is attached to the α carbon, the thermodynamic and electronic properties of intermediates derived from these two C_3 alcohols should be very different. In fact the thermodynamic (e.g., dehydrogenation equilibria) and electronic behavior of 1-propanol is much closer to that of ethanol than to that of 2-propanol, and so are the general reactions of aldehydes as opposed to ketones. Yet in the present system the β(N)/β(R) selectivities for the 1-propanol and 2-propanol condensations with the C_1 intermediate are close to each other and different from that for ethanol. Hence we consider the thermodynamic and electronic factors to be of secondary importance and the steric factors of primary importance in determining the β(N)/β(R) selectivity.

The C_4 product composition that resulted from the $C_3 + C_1$ addition over the Cs/Cu/ZnO catalyst rules out a CO insertion mechanism proposed by Mazanec (*7*). In particular, 2-propanol or acetone injection would be expected, by Mazanec's mechanism, to yield 2-methyl-1-propanol, a product that was not generated from 2-propanol over the Cs/Cu/ZnO catalyst (*31*). Thus the Cs/Cu/ZnO catalyst contrasts with a zirconia catalyst over which the synthesis of 2-methyl-1-propanol from acetone was reported (*32*), in support of Mazanec's mechanism. As the overall synthesis rates over the Cs/Cu/ZnO and related catalysts far exceed those over the ZrO_2 and related catalysts under comparable conditions, it is concluded that the alkali-promoted β addition is so far the most efficient chain growth mechanism in oxygenate synthesis.

To summarize the $C_3 \rightarrow C_4$ chemistry, we note that the synthetic patterns were systematically studied only over the most active Cs/Cu/ZnO catalyst, with the results

$$\beta(\mathrm{N}) \gtrsim \beta(\mathrm{R}) > \ell \quad \text{for } C_3 = \text{1-propanol}$$

and

$$\beta(\mathrm{R}) \approx \beta(\mathrm{N}) \gg \ell \quad \text{for } C_3 = \text{2-propanol.}$$

The significant contribution of the β(N) path is attributed to a steric hindrance of the stereoisomerization of the β-ketoalkoxide intermediate that favors the β(R) path in the $C_2 \rightarrow C_3$ step. Because 2-propanol is not a product of the native synthesis, as it has been injected for the purpose of elucidating the mechanism only, the dominant $C_3 \rightarrow C_4$ pathway is the β addition of the C_1 intermediate to that formed from 1-propanol to give 2-methyl-1-propanol. This alcohol is the most abundant C_4 product and one of the most abundant products of the whole synthesis.

$C_4 \rightarrow C_5$ synthesis. 1-Butanol, a minor product of the synthesis, continues the

chain growth path as evidenced by the presence of 2-methyl-1-butanol that originates by β addition (R = C_2H_5, R′ = R″ = H) and 1-pentanol that results from the linear growth step (cf. Table 2). 2-Methyl-1-propanol should give rise to $(CH_3)_3CCH_2OH$ by β addition β(N) or β(R). This alcohol with a tertiary carbon was not detected (cf. Table 2), and in general 2-methyl-1-alkanols do not add any further C_1 building blocks. This lack of β addition is a feature common with aldol synthesis that does not occur at a branched β carbon, as in Schemes I and II the substituent R would represent two methyl groups which render the carboanion $R_2CCHO^{\ominus}$ energetically inaccessible. Taking into account that the linear growth ℓ also does not occur with 2-methyl-1-propanol as discussed in Section B1, the synthesis ends at this β-branched alcohol, and in general at every 2-methyl-1-alkanol. Because 2-methyl-1-propanol is a major product of β addition to 1-propanol, also a major product, and all higher 2-methyl-1-alkanols are products of β additions to 1-alkanols that are minor products, the termination of the chain growth at 2-methyl-1-alkanols is the primary cause of 2-methyl-1-propanol being the dominant product of the synthesis.

$C_2 \rightarrow C_4$ synthesis. Two C_2 intermediates couple to 1-butanol by β(N) and to 2-butanol by β(R). 2-Butanol is the sole product of the β(R) coupling as is seen from the ^{13}C label locations at C-2 and C-4 upon injection of ^{13}C-1-labeled ethanol (cf. Tables 5 and 6). Hence, no portion of 2-butanol originates by 2-propanol + C_1 coupling because there is no prior path to 2-propanol, β or ℓ. 1-Butanol, however, originates both by C_2 + C_2 β(N) coupling, with ^{13}C labels from ^{13}C-1 ethanol at C-1 and C-3 of 1-butanol, and by C_3 + C_1 linear growth ℓ, with the ^{13}C label from the same source ending up at C-4 or C-3 of 1-butanol, depending on whether C-3 or C-2 of 1-propanol was enriched in the previous step. Inspection of Tables 5 and 6 shows that both the C_2 + C_2 β(N) and the C_3 + C_1 ℓ paths operate but the latter prevails at high temperatures, most likely due to the greater abundance of the C_3 and C_1 reactants even in the presence of the injected C_2 alcohol. Table 2 shows that in the native synthesis 1-butanol is approximately four times as abundant as 2-butanol, a result that is consistent with the C_3 + C_1 step being the main source of 1-butanol while the C_2 + C_2 addition is the sole source of 2-butanol.

C_3 + C_n (n = 2, 3) synthesis. These minor reaction pathways provide alternative routes to C_4 + C_1 and C_5 + C_1 reactions that yield 2-methyl-1-butanol, 2-methyl-1-pentanol, and 1-pentanol. The isotope distributions observed for 2-methyl-1-butanol, presented in Tables 5 and 6, clearly indicate that coupling of the C_2 + C_3 fragments is a pathway to its formation. For example, for 2-methyl-1-butanol synthesis over the Cs/Cu/ZnO catalyst at 553 K, the isotope distribution data suggest the reaction stoichiometry of

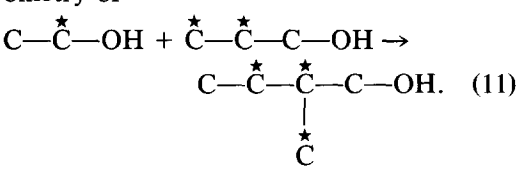

(11)

In addition, by employing the reaction principles of Schemes I and II, the formation of 3-methyl-2-butanol via C_3 + C_2 β(R), with R = R″ = CH_3, R′ = H, of 3-pentanol via C_3 + C_2 β(R), with R = R′ = H, R″ = C_2H_5, and of 1-pentanol via C_3 + C_2 β(N), with R = R′ = H, R″ = C_2H_5, can be predicted. In an analogous fashion the C_6 alcohols 2-methyl-3-pentanol and 2-methyl-1-pentanol can be obtained via C_3 + C_3 β(R) and C_3 + C_3 β(N), respectively, from precursors with R = CH_3, R′ = H, and R″ = C_2H_5. All of these products and their corresponding ketones and aldehydes were observed (cf. Table 2), and thus a full accounting of all of the C_5 and C_6 oxygenates has been made based on the two types of β additions, β(R) and β(N).

3. Aldehydes and ketones. The aldehydes and ketones that correspond to the observed alcohols were identified in the reaction product. Under the set of operating

conditions employed at temperatures above 573 K, the yields of these minor products were close to the equilibrium yields (*31*) for reaction stoichiometries

$$RCHO + H_2 \rightleftarrows RCH_2OH \quad (12)$$

and

$$RC(O)R' + H_2 \rightleftarrows RCH(OH)R'. \quad (13)$$

Similar equilibrium yields were observed for the methyl esters (*31*) consistent with the reaction stoichiometry

$$RCHO + CH_3OH \rightleftarrows RCOOCH_3 + H_2. \quad (14)$$

4. Methyl ester formation. The isotope distributions observed for the methyl esters (cf. Tables 7–9) are consistent with the two reactions generally proposed for their formation, i.e., the Tischenko and the Cannizaro reactions. The active C_1 intermediate is formaldehyde for the Cannizzaro reaction and methoxy for the Tischenko reaction as discussed by Vedage *et al.* (*6*). Based on both of these schemes, the ^{13}C isotope distribution of the acyl group of the methyl ester should be that of the parent alcohol and the ^{13}C isotope content of the methoxy carbon should be that of the methanol reactant, as is observed to be the case. An important feature of the Tischenko reaction is that the mechanism is S_N2 in nature, with attack of the methoxy oxygen on the C-1 carbon of the aldehydic species accompanied by loss of a hydride. Since $H^{\ominus}$ is a much stronger nucleophile than the $CH_3O^{\ominus}$ group, the Tischenko reaction is expected to be slow. However, this reaction may be facilitated by stabilization of $H^{\ominus}$ on the catalyst surface since the existence of hydride species on the surface of ZnO is well established (*17, 33, 34*).

C. Summary of the Reaction Pathways and the Effect of Cesium on Higher Oxygenate Synthesis

The patterns for synthesis of higher oxygenates from CO/H_2 over Cu/ZnO and Cs/Cu/ZnO catalysts are governed by the following features:

1. Linear growth ℓ that yields a C_{n+1} *primary* alcohol from a C_n ($n \geq 1$) *primary* alcohol.
2. Addition of C_1, C_2, and C_3 oxygenated fragments at the β carbon of a C_n ($n \geq 2$) alcohol to form C_{n+m} ($m = 1, 2, 3$) alcohols.
3. In the $C_n + C_1$ β additions, retention of oxygen associated with the C_1 fragment and rejection of oxygen associated with the C_n fragment by a process termed here *aldol coupling with oxygen retention reversal,* β(R).
4. In the same $C_n + C_1$ β additions, retention of oxygen associated with the C_n fragment and rejection of oxygen associated with the C_1 fragment by a process consistent with the normal course of aldol condensation and denoted here as β(N).
5. Absence of the β and ℓ chain growth steps for 2-methyl-1-alkanols.
6. Occurrence of aldehydes, ketones, and methyl esters that are derived from, and at high temperatures are at equilibrium with, their corresponding alcohols.

The role of cesium is to promote very significantly both the linear growth ℓ and the β additions in favor of the latter, and thereby increase the selectivity toward the principal branched product, 2-methyl-1-propanol. Of the two types of β additions β(N) and β(R), that with oxygen retention reversal β(R) entirely dominates the $C_2 \rightarrow C_3$ step over the Cs/Cu/ZnO catalyst at high temperatures. Both β(N) and β(R) types occur in the $C_n \rightarrow C_{n+1}$ ($n \geq 3$) additions, a feature that is likely to be caused by stereochemistry of the interactions of the C_{n+1} intermediate, bonded to the Cs^+ ions, with the catalyst surface.

Mechanistically, oxygenate coupling reactions appear to be of prime importance. The linear growth ℓ has been shown, for the $C_1 \rightarrow C_2$ step, to occur preferentially by coupling of oxygenated intermediates at α carbons rather than by CO insertion reactions (*2*), and the same mechanism is sug-

gested for all the $C_n + C_1$ ℓ synthetic steps. The β additions have all features of a reaction path involving β-ketoalkoxides in which the alkoxide oxygen is retained in the β(R) oxygen retention reversal reaction type and the keto oxygen in the β(N) normal aldol coupling type. The catalyst contains a hydrogenation component Cu/ZnO and a basic component, the latter effecting the oxygenate coupling reactions ℓ and β. Cesium acts as a strong base and the ZnO component as a weaker base, and it is proposed that their counterions enter the reaction cycle by nucleophilic attack of the carbonyl groups of aldehydes and ketones. If the β-ketoalkoxide bonded to the Cs^+ ions is free of substituents, the keto group can move freely to the hydrogenation component of the catalyst and the β(R) type dominates as in the $C_2 \rightarrow C_3$ step catalyzed by the Cs/Cu/ZnO catalyst. Methyl substituents at the backbone carbons of the β-ketoalkoxide sterically hinder the removal of the keto group from the coordination sphere of the Cs^+ ions and both types of β additions, β(R) and β(N), occur. Although the proposed mechanism involving the β-ketoalkoxide intermediate is more specific than the information contained in the isotope label flows and the product composition, it accounts entirely for all the observations that rule out the whole class of CO insertion mechanisms. Moreover, the mechanistic patterns permit a kinetic model to be set up for the whole oxygenate synthesis and to understand the molecular basis for the relative rates of the individual synthetic steps (*35*). In particular, the mechanistic effects of the cesium dopant reported here result in (β+ ℓ) rates for the $C_2 \rightarrow C_3$ step greater than for any other $C_n \rightarrow C_{n+1}$ steps, with the consequence that the synthesis generates a "bimodal" product distribution wherein maxima placed at C_1 (methanol) and i-C_4 (2-methyl-1-propanol) are separated by a minimum at C_2 (ethanol). As the overall rates of CO conversion are higher over the Cs/Cu/ZnO catalyst than over the Cu/ZnO catalyst, the Cs dopant produces both increased activity and increased selectivity toward the methanol/2-methyl-1-propanol mixtures.

ACKNOWLEDGMENTS

This work was supported in part by U.S. Department of Energy Contracts DE-FG22-83PC60786 and DC-AC22-84PC70021 and by Solar Energy Research Institute Subcontract XX-4-04019-01. C.E.B. is pleased to acknowledge the receipt of Buch, Horner, and Texaco Fellowships via the Lehigh University Chemistry Department.

REFERENCES

1. Nunan, J., Klier, K., Young, C. W., Himelfarb, P. B., and Herman, R. G., *J. Chem. Soc. Chem. Commun.*, 193 (1986).
2. Nunan, J. G., Bogdan, C. E., Klier, K., Smith, K. J., Young, C. W., and Herman, R. G., *J. Catal.* **113,** 410 (1988).
3. Klier, K., Young, C. W., and Nunan, J. G., *Ind. Eng. Chem. Fundam.* **25,** 36 (1986).
4. Fischer, F., and Tropsch, H., *Brennstoff. Chem.* **4,** 276 (1923).
5. Natta, G., Colombo, U., and Pasquon, T., *in* "Catalysis" (P. H. Emmett, Ed.), Vol. 5, Chap. 3. Reinhold, New York, 1957.
6. Vedage, G. A., Himelfarb, P. B., Simmons, G. W., and Klier, K., *Amer. Chem. Soc. Symp. Ser.* **279,** 295 (1985).
7. Mazanec, T. J., *J. Catal.* **98,** 115 (1986).
8. Biloen, P., Helle, J. N., and Sachtler, W. M. H., *J. Catal.* **58,** 95 (1979).
9. Ponec, V., and van Barneveld, W. A., *Ind. Eng. Chem. Prod. Res. Dev.* **18,** 268 (1979).
10. Wender, I., Levine, R., and Orchin, M., *J. Amer. Chem. Soc.* **71,** 4160 (1949).
11. Frolich, P. K., and Cryder, D. S., *Ind. Eng. Chem.* **22,** 1051 (1930).
12. Graves, G. D., *Ind. Eng. Chem.* **23,** 1381 (1931).
13. Morgan, G. T., Hardy, D. V. N., and Procter, R. H., *J. Soc. Chem. Ind. Trans. Commun.* **51,** IT (1932).
14. Fox, J. R., Pesa, F. A., and Curatolo, B. S., *J. Catal.* **90,** 127 (1984).
15. Bond, G. C., "Catalysis by Metals," p. 409. Academic Press, London/New York, 1962.
16. Thomas, C. L., "Catalytic Processes and Proven Catalysts," pp. 49–51, 139–141. Academic Press, New York, 1970.
17. Kokes, R. F., and Dent, A. L., *Adv. Catal.* **22,** 1 (1972).
18. Vedage, G., and Klier, K., *J. Catal.* **77,** 558 (1982).
19. Mokwa, W., Kohl, D., and Heiland, G., *Fresenius Z. Anal. Chem.* **314,** 315 (1983).
20. Cunningham, J., Al-Sayyed, G. H., Cronin, J. A.,

Fierro, J. L. G., Healy, C., Hirschwald, W., Ilyas, M., and Tobin, J. P., *J. Catal.* **102,** 160 (1986).
21. Elliott, D. J., and Pennella, F., *Prepr. Div. Pet. Chem. ACS* **31**(1), 39 (1986).
22. Herman, R. G., Klier, K., Simmons, G. W., Finn, B. P., Bulko, J. B., and Kobylinski, T. P., *J. Catal.* **56,** 407 (1979).
23. Himelfarb, P. B., Simmons, G. W., Klier, K., and Herman, R. G., *J. Catal.* **93,** 442 (1985).
24. Herman, R. G., *in* "Catalytic Conversions of Synthesis Gas and Alcohols to Chemicals" (R. G. Herman, Ed.), p. 433. Plenum, New York, 1984.
25. Dietz, W. A., *J. Gas Chromatogr.* **5,** 68 (1967).
26. Herman, R. G., Pendleton, P., and Bulko, J. B., *in* "Advances in Materials Characterization" (D. R. Rossington, R. A. Condrate, and R. L. Snyder, Eds.), p. 109. Plenum, New York, 1983.
27. Bulko, J. B., Herman, R. G., Klier, K., and Simmons, G. W., *J. Phys. Chem.* **83,** 3118 (1979).
28. Vedage, G. A., Pitchai, R., Herman, R. G., and Klier, K., *in* "Proceedings, 8th International Congress on Catalysis," Vol. II, p. 47, 1984.
29. Smith, K. J., and Anderson, R. B., (*a*) *Canad. J. Chem. Eng.* **61,** 40 (1983); (*b*) *J. Catal.* **85,** 428 (1984).
30. Morrison, R. T., and Boyd, R. N., "Organic Chemistry," 4th ed., p. 222. Allyn & Bacon, Boston, 1983.
31. Young, C. W., Ph.D. dissertation, Lehigh University, 1987.
32. Silver, R. G., Tseng, S. C., and Ekerdt, J. G., *Prepr. Div. Fuel Chem. ACS* **31**(3), 11 (1986).
33. Eischens, R. P., Pliskin, W. A., and Low, M. J. D., *J. Catal.* **1,** 180 (1962).
34. Dent, A. L., and Kokes, R. J., *J. Phys. Chem.* **73,** 3781 (1969).
35. Smith, K. J., Young, C. W., Herman, R. G., and Klier, K., to be published.